Functional characterization of NAC-domain transcription factors implicated in control of vascular cell differentiation in *Arabidopsis* and *Populus*

By

Emily H. Grant

Thesis submitted to the faculty of the Virginia Polytechnic Institute and State University in partial fulfillment of the requirements for the degree of

MASTER OF SCIENCE

in

Forestry

APPROVED:

Dr. Amy M. Brunner, Chair

Dr. Eric P. Beers, Co-Chair

Dr. James G. Tokuhisa

Dr. James Westwood

December 10, 2008
Blacksburg, VA

Keywords: ***Arabidopsis thaliana, Populus trichocarpa,*** **xylem, NACs, transcription factor, wood**

Functional characterization of NAC-domain transcription factors implicated in control of vascular cell differentiation in *Arabidopsis* and *Populus*

By

Emily H. Grant

Dr. Amy M. Brunner, Chair

Department of Forestry

(Abstract)

Wood has a wide variety of uses and is arguably the most important renewable raw material. The composition of xylem cell types in wood determines the utility of different types of wood for distinct commercial applications. Using expression profiling and phylogenetic analysis, we identified many xylem-associated regulatory genes that may control the differentiation of cells involved in wood formation in *Arabidopsis* and poplar. Prominent among these are NAC-domain transcription factors (*NAC*s). In addition to their roles as regulators of xylem differentiation, *NAC*s are regulators of meristem development, organ elongation and separation. We studied a subset of *Populus* and *Arabidopsis NAC*s with putative involvement in xylem cell expansion and elongation (*XND1*/*ANAC104*, *PopNAC118*, *PopNAC122*, *PopNAC128*, *PopNAC129*), and secondary cell wall synthesis (*ANAC073*, *PopNAC105*, *PopNAC154*, *PopNAC156*, *PopNAC157*). Using quantitative Real-Time PCR, we evaluated expression of the selected *Populus NAC*s in a developmental gradient and in response to bending stress. We prepared transgenic *Arabidopsis* and *Populus* plants with increased or decreased expression of select *NAC* genes. For dominant repression of target gene expression, we evaluated transgenic plants expressing translational fusions of NAC-EAR (ERF amphiphilic repressor) chimeras through chimeric repressor silencing-technology (CRES-T). *XND1* overexpression in *Populus* and *Arabidopsis* resulted in severe stunting and suppression of xylem differentiation. Overexpression of *PopNAC122*, an *XND1* ortholog, yielded an analogous phenotype in *Arabidopsis*. *Populus XND1* overexpressors lacked phloem fibers and showed a reduction in cell size and number, vessel number and frequency of rays. Knowledge gained through characterization of these wood-associated regulatory genes can be used to optimize molecular breeding and genetic engineering strategies for improved wood quality and increased biomass.

Acknowledgements

I would like to sincerely thank my advisors, Dr. Eric Beers and Dr. Amy Brunner, for their guidance, advice and support during my graduate research project. I would also like to express my appreciation to my committee members Dr. James Tokuhisa and Dr. James Westwood for their suggestions and guidance. I would like to thank the coordinators of the Molecular Plant Sciences program.

I would like to thank Dr. Takeshi Fujino and Dr. Chengsong Zhao for their technical assistance and excellent scientific advice. I would also like to thank Dr. Zhengxing Shen, Earl Petzold and Shelley Moore for their assistance in this project. Thanks to Xiaoyan Sheng and Elizabeth Etherington for all of their technical support.

Many thanks to my parents, Frank Hurst Sr. and Norma Hurst, for their support throughout my college and graduate education. I would also like to thank my brother, Dr. Frank Hurst Jr., for all of his advice and encouragement. I want to express my sincere appreciation to my husband, Jeffrey Grant, for his unwavering support during my graduate research and for accompanying me in many evening and weekend trips to the lab.

Funding for this research was provided by the Department of Energy, Office of Science, Office of Biological and Environmental Research (Grant No DE-FG02-06ER64185). Attendance to the IUFRO 2007 Forest Biotechnology conference was supported by the Graduate Student Association Travel Fund Program of Virginia Tech and by the Department of Energy, Office of Science, Office of Biological and Environmental Research (Grant No DE-FG02-06ER64185).

Table of Contents

List of Figures

List of Tables

Chapter 1

Introduction

Wood is an important, renewable raw material with many uses such as lumber, paper, fiberboard, and engineered wood products. These products were estimated to value $243 billion in U.S. sales in 2005 (DOE). Additionally, $350 billion is contributed annually to the world's economy by wood and paper products industries (FAO, 2005). The development of strategies for modifying wood characteristics and increasing wood biomass is central to the domestication of forest trees. Modification of trees for optimization of wood production has the potential to produce high-yielding, intensively-managed plantations that occupy a small amount of land. Domestication for optimum wood production should be achievable without detracting from the traditional environmental benefits provided by forests including carbon sequestration, watershed protection, improved air quality and recreational and wildlife habitats.

Trees are characterized by their extensive formation of secondary xylem which is both a supportive and conductive tissue. *It is the composition of xylem, i.e. the structure, arrangement and relative proportions of the specialized xylem cell types, that determines the physical properties of woods and hence their suitability for specific commercial applications* (Esau, 1965). Alterations for optimal wood yield depend on attaining knowledge of gene function and regulatory pathways related to secondary xylem formation. Gene and genome duplications and subsequent gene subfunctionalization may represent the underlying mechanisms through which genes and regulatory pathways involving wood formation have evolved. The model herbaceous annual *Arabidopsis* and the model woody perennial poplar represent complementary models for revealing the genetic pathways regulating secondary xylem formation. A small number of genes controlling xylem formation and secondary cell wall synthesis have already been characterized in *Arabidopsis* and have clear orthologs in poplar. Moreover, the gene expression patterns of some of the poplar orthologs suggests that they also function in xylem development. In an effort to translate findings from studies in *Arabidopsis* to an

industrial crop, we studied the function of selected NAC-domain transcription factors that are putative key regulators of the differentiation of xylem in poplar.

Arabidopsis offers experimental advantages such as a fully annotated genome sequence and rapid growth and development. However, studies with a model tree such as poplar are vital to understanding aspects of wood formation not represented in *Arabidopsis*. Studying wood formation in trees offers a more economically relevant viewpoint due to complex seasonal changes, age-related maturation, reaction wood, heartwood and specialized cell types of long-lived perennials. Trees also provide a notably larger amount of cambial tissue for study relative to annuals such as *Arabidopsis*. Considering the availability of the genome sequence and the possibility of identifying members of gene families orthologous to *Arabidopsis NAC* genes, poplar is a valuable model that also offers facile transformation and early, rapid growth compared with other trees.

Xylem in dicotyledonous, woody plants is comprised of both vertical and horizontal tissues. The vertical, or axial, component consists of three specialized cell types. Non-living vessel members and tracheids, collectively referred to as tracheary elements (TEs), serve to conduct water. Fibers provide support while parenchyma cells provide storage and food translocation. Parenchyma cells also form the ray, or horizontal, component of xylem. There are three common phases involved in the formation of TEs and fibers: 1) cambium cell division, 2) cell elongation and/or expansion, and 3) secondary cell wall synthesis. TEs progress through a fourth step of differentiation, programmed cell death (PCD).

NAC-domain transcription factors (*NAC*s) are important to regulation of several aspects of plant development including root formation, flower maturation, organ separation and meristem formation. NAC proteins are plant-specific transcriptions factors containing a highly conserved N-terminal sequence designated the NAC domain and a divergent C-terminus (Souer et al., 1996; Riechmann et al., 2000). The NAC name is derived from the *NO APICAL MERISTEM* (*NAM*) gene from petunia and the *Arabidopsis* genes *ATAF1/ATAF2* and *CUP-SHAPED COTYLEDON2* (*CUC2*) (Aida et al., 1997). The

NAC domain contains five subdomains referred to as A to E (Kikuchi et al., 2000). There are approximately 105 NAC proteins in the *Arabidopsis* genome (Ooka et al., 2003; Olsen et al., 2005). *Arabidopsis cuc1/cuc2* double mutants lack an embryonic shoot apical meristem, and their cotyledons are fused to form a "cup"; whereas *cuc3* mutants have fused floral organs in addition to fused cotyledons (Aida et al., 1997; Takada et al., 2001; Vroemen et al., 2003). Genes belonging to two subgroups of *Arabidopsis NAC* genes have been characterized as regulators of xylem differentiation. In separate studies, it was shown that overexpression of genes in related subgroups, *NST1* and *NST2* (Mitsuda et al., 2005) and *VND6* and *VND7* (Kubo et al., 2005), led to ectopic formation of TE-like cells. Ectopic formation of the TE-like cells was coupled with expression of markers for secondary cell wall biosynthesis for both *VND7* and *NST1*. For *VND6/7*, the formation of xylem cells occurred without an increase in cell size implying that *VNDs* do not regulate xylem cell enlargement. Based on the results from these studies, it is evident that a central element of wood formation--secondary cell wall synthesis--can be influenced via manipulation of a single NAC-domain transcription factor.

Of the 105 NAC-domain genes in the *Arabidopsis* genome, 16 are expressed in vascular tissues (Kubo et al., 2005; Mitsuda et al., 2005; Zhao et al., 2005). Only one of these genes is linked to phloem-cambium (PC) development (Zhao et al., 2005). Of the 15 remaining xylem-associated *NAC* genes, members of the *VND* and *NST* subgroups account for ten. Zhao et al. (2005) studied the *NAC* gene exhibiting the highest expression in xylem. Based on gain- and loss-of-function studies, *XYLEM NAC DOMAIN 1* (*XND1*, At5g64530) appears to be a negative regulator of secondary cell wall synthesis and PCD, i.e. terminal differentiation, in xylem in contrast with the *VND*s and *NST*s which act to promote secondary cell wall synthesis. *xnd1* plants produced shorter fibers and TEs resulting in moderately shorter plants (Zhao et al., 2008). In contrast, plants overexpressing *XND1* were severely stunted and in the most extreme cases TE differentiation was completely blocked as evidenced by the complete lack of secondary cell wall thickenings (Zhao et al., 2008). *Pro*$_{35S}$*:XND1* plants also lacked expression of selected TE markers and did not transport Evans blue throughout the vascular system. Evans blue is a vital stain excluded from living cells but readily taken up by dead xylem

cells. That normal patterns of expression were observed for several phloem markers in *XND1* overexpressors lacking xylem, suggested that the inhibitory effects of *XND1* overexpression were restricted to xylem cells (Zhao et al., 2008). RT-PCR results showed that the severity of stunting and xylem discontinuity was positively correlated with the level of *XND1* transcript. *XND1* knockouts (two independent alleles) with confirmed transposon insertions lacked detectable *XND1* transcript levels and exhibited a reduction in plant stature by as much as one-third, compared to wild-type (WT) plants (Zhao et al., 2008). The lengths of fibers, vessel members, siliques and leaves were significantly reduced in the *XND1* knockout plants compared to WT. Based on the results from both gain- and loss-of-function experiments, it appears that *XND1* indirectly facilitates cell enlargement by blocking secondary cell wall synthesis and PCD. An antagonistic relationship may exist between *XND1* and *VND/NST* family members, coordinating the timing of cell expansion with secondary cell wall synthesis and PCD in xylem.

These findings regarding the *VND*/*NST* and *XND1* NAC-domain transcription factors and their effects on xylem differentiation make a strong case for functional analysis of as yet uncharacterized xylem-associated *NAC*s in *Arabidopsis* and other important models. Here we show that there are putative orthologous poplar *NAC*s upregulated in vascular tissues. We used a combination of annotated genome sequence data (Tuskan et al., 2006) and oligo-based microarray resources recently developed for poplar (Brunner et al., unpublished).

The poplar genome contains approximately 157 *NAC* genes which is 1.5 times more than in *Arabidopsis* and 2 times more than in rice (S. Covert pers. comm.). Genome duplications are responsible for the expansion in the number of transcription factors in *Arabidopsis* (Maere et al., 2005), and the same appears to be true for poplar, with a 60% retention rate since the most recent genome duplication (Tuskan et al., 2006). Transcript profiling of a variety of poplar tissue types and developmental stages using a whole-genome NimbleGen oligonucleotide microarray identified poplar *NAC* genes upregulated in xylem or PC (Brunner et al., unpublished). Profiling of six tissue types has been completed: xylem, PC, female catkin, male catkin, seed and germinant.

In order to study the putative functions of select *Populus NAC* (*PopNAC*) genes, we used Real-Time PCR to show tissue- and organ-specific expression in a developmental continuum. Expression of the *NAC* genes in *Populus* individuals undergoing normal development and plants subjected to treatment-induced reaction (or tension) wood formation was evaluated. Researchers study reaction wood in trees to investigate the molecular pathways involved in wood development (Hellgren et al., 2004). Tension wood occurs on the stretched surface of the bent stem and is characterized by enhanced growth, a reduction in vessel element frequency and size and a 10-20% increase in cellulose content corresponding with a decrease in lignification (Hellgren et al., 2004; Andersson-Gunneras et al., 2006). In opposite wood forming on the compressed side of the bend, there is an increase in lignin content coupled with a decrease in cellulose as well as an inhibition in cambial cell division (Andersson-Gunneras et al., 2006). One *PopNAC*, *PopNAC154*, is putatively involved in wood formation; it exhibited an increase in transcription in tension wood in contrast to opposite wood (Andersson-Gunneras et al., 2006).

We chose eleven genes – three from *Arabidopsis* and eight from poplar – to study due to their putative roles in the developmental continuum of xylem cell differentiation. The overall objective was to characterize select vascular-associated *NAC*s as putative regulators of secondary growth in both *Arabidopsis* and *Populus*. Functional redundancy of genes can mask single-gene recessive loss-of-function phenotypes. To circumvent the technical challenge, we employed ERF amphiphilic repressor (EAR) (Ohta et al., 2001) motif-mediated dominant repression of target gene expression through translational fusions of the selected *NAC* genes to an EAR domain, LDLDLELRLGFA, termed SRDX, for expression (Hiratsu et al., 2003). The motif was placed as an in-frame fusion attached to the C-terminus of select *NAC*s and cloned into a binary vector for 35S-driven expression of NAC-EAR fusions. Select *Arabidopsis* and *Populus NAC* genes were amplified and inserted into cloning vectors for both overexpression and dominant repression studies. Constructs for select genes were transformed for misexpression in *Arabidopsis* and *Populus*.

Chapter 2: Functional analysis of XND1 in *Arabidopsis*

2.1 Introduction

Studies of the 105 NAC-domain transcription factors in *Arabidopsis* have revealed involvement in various developmental stages from cotyledon development (Aida et al., 1997; Takada et al., 2001; Vroemen et al., 2003) to tracheary element differentiation and PCD (Kubo et al., 2005; Mitsuda et al., 2005; Zhao et al., 2008). Of the 16 vascular-associated NAC-domain transcription factors in *Arabidopsis* (Zhao et al., 2005), *VND6/7* and *NST1/2/3* have been characterized as promoters of xylem differentiation (Kubo et al., 2005; Mitsuda et al., 2005; Mitsuda et al., 2007). In contrast, the most highly expressed xylem-associated *NAC* gene, *XND1* (At5g64530), has been implicated as a negative regulator of secondary wall synthesis and PCD (Zhao et al., 2005; Zhao et al., 2008). Due to functional redundancy exhibited by the *VND* and *NST* subgroups, it has been shown that overexpression of NAC-SRDX fusions leads to phenocopies of multigene knockouts (Kubo et al., 2005; Mitsuda et al., 2005). Based on these findings, we employed an XND1-SRDX fusion as well as a series of domain swapping experiments to further characterize the function of XND1 in *Arabidopsis*.

2.2 Materials and Methods

2.2.1 Overview of cloning and transformation

Standard recombinant DNA techniques were employed to amplify and manipulate DNA by first utilizing the pGEM–T Easy Vector system (pGEM) (Promega Corp. Madison, WI) as a shuttle vector. The recombinant DNA was subsequently cloned into the appropriate binary vector. $Vent_R^{®}$ proofreading polymerase (New England Biolabs, Ipswich, MA) was used to amplify gene coding regions of the selected *NAC* genes by PCR. Depending on the expression of a particular gene, gene coding regions were amplified from *Arabidopsis* xylem or bark/phloem cDNA libraries (Zhao et al., 2000). RNA extraction was accomplished with the use of RNeasy Plant Mini Kit and protocol

(Qiagen Inc., Valencia, CA). RT-PCR was carried out according to the RETROscript Kit instruction manual (Ambion, Austin, Texas) in a 25 µl standard reaction with primers specific to each gene.

Restriction sites were added at the amplification step to enable the excision of the cDNA fragments from the pGEM vector for cloning into the appropriate binary vector. Based on PCR results, gel extraction was necessary in some cases and was accomplished using the QIAEX II Gel Extraction kit (Qiagen Inc., Valencia, CA). Transformations of *Escherichia coli* (*E. coli*) strain DH5α cells were conducted as outlined in the technical manual for the pGEM vector system. Plasmid DNA was isolated from *E. coli* for sequence confirmation through the use of QIAprep Spin Miniprep kit (Qiagen Inc., Valencia, CA). All sequencing was performed by the Core Laboratory Facility, Virginia Bioinformatics Institute, Blacksburg, VA. Transformation of the assembled constructs was accomplished by insertion of recombinant plasmid DNA into *Agrobacterium tumefaciens* (*Agrobacterium*) strains GV3101 and AGL1 according to the outlined method in Chen et al. (1994) with the exception of the liquid nitrogen freezing step being replaced by a heat shock step in which the cells were placed in a 37˚C water bath for one minute followed immediately by incubation on ice for two minutes. 0.8 ml of 2XTY was added to tubes containing transformed cells followed by incubation of the mixture at 28˚C with shaking at 250 rpm for two hours. Transformed cells were pelleted by centrifugation at 5,000 rpm for 30 seconds and resuspended in 100 µl 2XTY. Remaining solution was spread onto an LB media plate containing the appropriate antibiotics for GV3101 (kanamycin, rifampicin, gentamicin) or AGL1 (kanamycin, carbenicillin, rifampicin).

2.2.1.1 Vectors

The binary vector pFGC5941, (http://www.arabidopsis.org/servlet/TairObject?id=500300075&type=vector) which confers BASTA resistance through the "bar" gene in plants, was utilized for all constructs. The insertion point was downstream of the CaMV 35S (Pro_{35S}) promoter, which has proven useful in determining gene function in both gain- and loss-of-function

studies (Xie et al., 2000; Takada et al., 2001; Hibara et al., 2003; Kubo et al., 2005; Mitsuda et al., 2005).

2.2.1.2 Constructs

NAC Gain- and Loss-of-Function Constructs

Pro_{35S}:XND1-SRDX

The preparation of the *XND1-SRDX* construct is described in Zhao et al. (2008).

Pro_{35S}:VND7-SRDX

The *Pro_{35S}:VND7-SRDX* construct is described in Zhao et al. (2008).

Pro_{35S}:ANAC073-SRDX

The coding region for At4g28500 (without the stop codon) was amplified from the xylem cDNA library (Zhao et al., 2000) using a sense *Xho* I linker primer, *ANAC073-S*, and a *Swa* I linker primer, *ANAC073-AS* (Appendix Table I). The PCR product was cloned into pGEM. pGEM-*ANAC073* was digested with *Sph* I and *Swa* I and cloned into pGEM-*SRDX* previously digested with *Sph* I and *Sma* I. After sequence verification, the *ANAC073-SRDX* fragment was digested with *Xho* I/*Swa* I and cloned into the pFGC5941 vector previously digested with *Xho* I/*Sma* I.

Pro_{35S}:ANAC073

The coding region for At4g28500 was amplified from an *Arabidopsis* xylem cDNA library (Zhao et al., 2000) using a sense *Xho* I linker primer, *ANAC073-S,* and an *Eco*R V linker primer, *ANAC073-3* (Appendix Table I). The PCR product was cloned into pGEM. After sequence verification, the *ANAC073* fragment containing the stop codon was digested out of pGEM with *Xho* I and *Eco*R V for ligation into the binary vector, pFGC5941, previously digested with *Xho* I and *Sma* I. The resulting construct was transformed into AGL1 and GV3101.

Pro_{35S}:ANAC096-SRDX

The coding region for At5g46590 (without the stop codon) was amplified from *Arabidopsis* cDNA using a sense *Sal* I linker primer, *ANAC096-S*, and a *Swa* I linker primer, *ANAC096-AS* (Appendix Table I). The resulting PCR product was cloned into pGEM. After sequence verification, the coding region of *ANAC096* was digested with *Sph* I and *Swa* I for ligation into the pGEM-*SRDX* vector previously digested with *Sph* I and *Sma* I. The *ANAC096-SRDX* in-frame fusion was confirmed by sequencing and digested from pGEM with *Sal* I and *Swa* I for ligation into the pFGC5941 vector previously digested with *Xho* I and *Sma* I. The construct was transformed into *Agrobacterium* GV3101 for transformation into *Arabidopsis*.

Pro_{35S}:ANAC096

The coding region for At5g46590 was amplified from *Arabidopsis* cDNA using a sense *Sal* I linker primer, *ANAC096-S*, and an *EcoR V* linker primer, *ANAC096-3* (Appendix Table I). The resulting PCR product was cloned into pGEM for sequence verification. The *ANAC096* coding region was digested out of pGEM with *Sal* I and *Eco*R V for ligation into the binary vector, pFGC5941, previously digested with *Xho* I and *Sma* I. This construct has been transformed into AGL1 and GV3101 *Agrobacterium* strains.

NAC Domain Swapping Constructs

In order to test the hypothesis that the C-terminus of XND1 acts as a repressor, we prepared domain swapping constructs. As a control for any *VND7* gene-specific effects from the activation domain, we prepared a construct containing the Herpes Simplex Virus VP16 activation domain (provided by J. McDowell). Schematics of the constructs are shown in Figure 1.

Pro_{35S}:XND1N5-VND7AD

The XND1 NAC domain (A-E or N1-N5) was amplified using ExTaq™ polymerase (Takara Bio USA, Madison, WI) from the *Pro_{35S}:XND1* construct using an *Xho* I linker primer, *XND1N5-S*, and a *Pvu* II linker primer, *XND1N5-AS* (Appendix Table I). The VND7 activation domain (C-terminus excluding the NAC domain) was amplified with ExTaq™ polymerase from the pGEM-*VND7* construct using an *Hpa* I linker primer,

VND7AD-S, and an *Eco*R V linker primer, *VND7AD-AS* (Appendix Table I). Both fragments were subsequently ligated into pGEM for sequencing. pGEM-*XND1N5* was digested with *Xho* I/*Pvu* II and in a separate reaction with *Xho* I/*Spe* I. pGEM-*VND7AD* was digested with *Hpa* I/*Spe* I. A three-piece ligation was performed using the 3000 base pair (bp) fragment from the *Xho* I/*Spe* I digestion of pGEM-*XND1N5*, the 500 bp fragment from the *Xho* I/*Pvu* II digestion of pGEM-*XND1N5* and the 300 bp fragment from the pGEM-*VND7AD* digestion. The *XND1N5-VND7AD* fragment was excised from pGEM by an *Xho* I/*Eco*R V digestion and ligated into pFGC5941 previously digested with *Xho* I/*Sma* I. For *XND1* cloning, the final glutamine (Q) residue was changed from CAA to CAG. For *VND7*, the initial asparagine (N) was changed from AAT to AAC. Neither nucleotide substitution resulted in an amino acid change.

Pro_{35S}:XND1N5-VP16

The XND1 NAC domain was amplified according to the description above. The Herpes Simplex Virus VP-16 activation domain was amplified using a *Sfo* I linker primer, *VP16AD-S* (Appendix Table I) and an *Eco*R V linker primer, *VP16AD-AS* (Appendix Table I) from a pTA7001 *Agrobacterium* stock. The resulting fragment was ligated into pGEM. pGEM-*XND1N5* was digested with *Xho* I/*Pvu* II and in a separate reaction with *Xho* I/*Spe* I. pGEM-*VP16AD* was digested with *Sfo* I and *Spe* I. A 3-piece ligation was performed using the ~3000 bp fragment from the *Xho* I/*Spe* I digestion of pGEM-*XND1N5*, the ~500 bp fragment from the *Xho* I/*Pvu* II digestion of pGEM-*XND1N5* and the ~300 bp fragment from the *Sfo* I/*Spe* I digestion of pGEM-*VP16AD*. The *XND1N5-VP16AD* fragment was excised from pGEM by an *Xho* I/*Eco*R V digestion and ligated into pFGC5941 previously digested with *Xho* I/*Sma* I. As described above, there was a single nucleotide change in *XND1N5*.

Pro_{35S}:VND7-XND1C

The XND1 c-terminus was amplified from *Pro_{35S}XND1*-pFGC5941 (provided by C. Zhao) with an *Hpa* I linker primer, *XND1C-S* (Appendix Table I), and an *Eco*R V linker primer, *XND1-02* (Appendix Table I). The coding region of *VND7* was digested from pGEM-*VND7* with *Sph* I/*Eco*R V and was ligated with pGEM-*XND1C*, previously

digested with *Sph* I/*Hpa* I. The *VND7-XND1C* fragment was digested from pGEM with *Xho* I/*Eco*R V and ligated into pFGC5941 binary vector, previously digested with *Xho* I/*Sma* I.

2.2.1.3 Transformation

Arabidopsis thaliana ecotype Columbia was used for all transformations. Transformation of *Arabidopsis* with *Agrobacterium* containing the appropriate construct was accomplished by the floral dip method (Clough and Bent, 1998). Transformants were selected by spraying seven-day-old plants with Finale (BASTA) herbicide (active ingredient, Glufosinate ammonium 0.03%) followed by re-application one week later.

2.2.2 Analysis of *Arabidopsis NAC* Transgenics

2.2.2.1 Microscopy

Pro$_{35S}$:PopNAC122 plants were grown alongside plants transformed with *Agrobacterium* containing only the pFGC5941 vector (vector-only control) for four weeks under a 14h/10h day/night cycle at 21-22˚C. Images were captured of herbicide-resistant T_2 plants exhibiting a dwarf phenotype and vector-only controls for characterization using Zeiss Axioimager M1 and Stemi SV11 microscopes (Carl Zeiss, Inc., http://www.zeiss.com/).

2.3 Results

XND1, a member of the NAC domain family in *Arabidopsis thaliana*, negatively regulates lignocellulose synthesis and programmed cell death in xylem

Chengsong Zhao[1], Utku Avci[2], Emily H. Grant[1,3], Candace H. Haigler[2,4] and Eric P. Beers[1],*

[1]Department of Horticulture, Virginia Polytechnic Institute and State University, Blacksburg, VA 24061, USA,
[2]Department of Crop Science, North Carolina State University, Raleigh, NC 27695, USA,

[3]Department of Forestry, Virginia Polytechnic Institute and State University, Blacksburg, VA 24061, USA, and
[4]Department of Plant Biology, North Carolina State University, Raleigh, NC 27695, USA

*Corresponding author
Telephone: 540-231-3210
Fax: 540-231-3083
E-mail: ebeers@vt.edu

This chapter was published in the *Plant Journal*, February 2008 and copyright is held by the authors with distribution and reproduction rights held by the journal. The *Pro$_{35S}$:XND1-SRDX* and *Pro$_{35S}$:VND7-SRDX* constructs and characterization (Figure S10; Zhao et al., 2008) were my contributions to this manuscript.

ANAC073 and *ANAC096* constructs

No informative phenotypes were observed for transformations with *ANAC073* and *ANAC096* overexpression and SRDX constructs. No transformants were recovered for *ANAC073-SRDX*.

Domain-Swapping

Given that the stunted, dark green phenotype of *Pro$_{35S}$:XND1-SRDX* plants was the same as that of the *Pro$_{35S}$:XND1* plants (Zhao et al., 2008), we transformed *Arabidopsis* with domain swapping constructs to determine the function of the XND1 C-terminus (Fig. 1). *Pro$_{35S}$:XND1N5-VND7AD* and *Pro$_{35S}$:VND7-XND1C* transgenic plants exhibited normal phenotypes. *Pro$_{35S}$:XND1N5-VP16* transgenics phenocopied *Pro$_{35S}$:XND1* plants (data not shown).

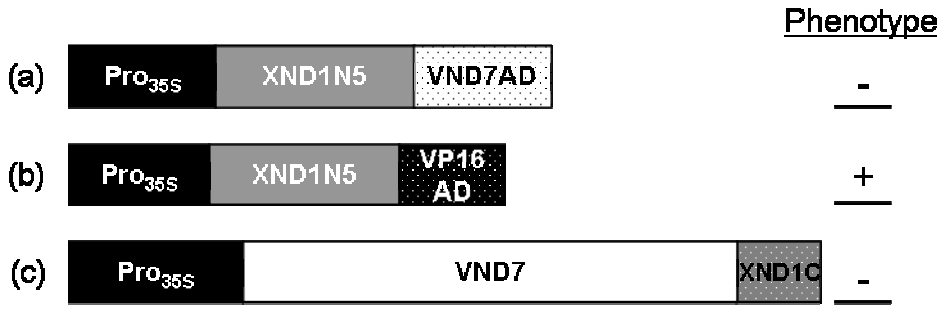

Figure 1. Schematic depicting constructs employed in the domain swapping experiment. All constructs are shown under the control of the 35S Promoter (*Pro$_{35S}$*).
(a) NAC domain of XND1 with the VND7 activation domain replacing the C-terminus of XND1. (b) The NAC domain of XND1 fused with the VP16 activation domain from Herpes Simplex virus replacing the C-terminus of XND1. (c) The full length VND7 coding region fused to the XND1 C-terminus. Column at right indicates the presence (+) or absence (-) of phenotype differing from wild-type.

2.4 Discussion

Plants transformed with *ANAC073* and *ANAC096* recombinant vectors did not show obvious phenotypes differing from WT. Both poplar and *Arabidopsis* tranformations using *ANAC073-SRDX* produced no transgenics. Further research is necessary to elucidate the function of these two *Arabidopsis NAC*s.

Overexpression of *XND1* leads to stunting and tracheary element discontinuity in *Arabidopsis* (Zhao et al., 2008). The addition of the SRDX repression domain to the coding region of XND1 did not alter the phenotype seen in *XND1* overexpressors (Zhao et al., 2008), which is different from the results observed in the fusion of SRDX with other *NAC* genes (Kubo et al., 2005; Mitsuda et al., 2005). Due to this unexpected result, we hypothesized that the C-terminus of XND1 may normally function as a transcriptional repressor, thus rendering the SRDX domain redundant. To test this hypothesis, we constructed a recombinant version of XND1 where the N-terminal DNA binding domain was fused to the powerful activation domain VP16 (Cress and Triezenberg, 1991) to the NAC DNA-binding domain of *XND1*. When overexpressed, this fusion resulted in a phenocopy of the *XND1* overexpressors. Moreover, when fused to VND7, the C-terminal domain of XND1 did not act as a dominant repressor of VND7 activity as reported for *VND7-SRDX* fusions (Kubo et al., 2005). Taken together, these results indicate that XND1 functions as a transcriptional activator, not a repressor. This speculation fails to provide an explanation for the lack of phenotypes observed for *Pro$_{35S}$:XND1N5-VND7AD* plants. One would expect to see *Pro$_{35S}$:XND1* phenocopies resulting from transformation with the *Pro$_{35S}$:XND1N5-VND7AD* construct if the XND1 C-terminus is

indeed an activation domain. It is possible that the VND7 activation domain is not as powerful as the VP16 activation domain.

We examined the amino acid sequence in the C-terminus of XND1 to identify motifs typically present in an activation domain. An acidic activation domain such as the VP16 activation domain is characterized by acidic amino acids flanking hydrophobic or aromatic residues (Cress and Triezenberg, 1991). The minimal activation domain of VP16 consists of six bulky hydrophobic residues interspersed with acidic residues (Cress and Triezenberg, 1991). The C-terminus of XND1 is leucine-rich and contains 13 acidic residues out of the total 32 amino acids. There is a region in the C-terminus in which a leucine is flanked by aspartate and glutamate residues, which suggests that the XND1 C-terminus may be an activation domain. Sainz et al. (1997) concluded that although the presence of certain hydrophobic residues has been shown to be essential for an activation domain, a low level of conservation exists in the regions containing those hydrophobic residues. In a yeast reporter activation experiment, Zhao et al. found that the XND1 C-terminus functioned as an activation domain in yeast (unpublished). Interestingly, the XND1 C-terminus shares a high degree of identity with *CYCD3;1*, specifically in the putative retinoblastoma binding domain (Huntley et al., 1998). *CYCD3;1* is involved in the initiation of the transition from G1 to S phase in the cell cycle (Huntley et al., 1998). Overexpression of *CYCD3;1* in transgenic plants led to the transition of cells into the S phase resulting in abnormal differentiation, in which poorly differentiated cells were formed due to persistent cell division (Menges et al., 2006). Sequence identity shared between the putative C-terminal activation domain in XND1 and the retinoblastoma binding domain in *CYCD3;1* suggests a common mechanism and may provide an explanation for the PCD inhibition observed in *XND1* overexpressors. Further research will focus on determining the function of the C-terminus of XND1, which will hopefully clarify why the fusion of the XND1 NAC domain to SRDX did not elicit a novel phenotype different from *Pro$_{35S}$:XND1*.

Chapter 3: Expression profiling of two *NAC* subfamilies associated with vascular tissue in *Populus*

3.1 Introduction

Genome duplications (Maere et al., 2005; Tuskan et al., 2006) have resulted in the expansion of *NAC* gene families in *Arabidopsis* and *Populus*. While *Arabidopsis* has 105 NAC genes, poplar contains approximately 157, which is twice the number of NAC genes found in rice. Transcript profiling in vascular tissue via microarray has facilitated the identification of poplar *NAC*s upregulated in xylem and PC (Brunner et al., unpublished). Based on microarray data and phylogenetic analyses, we chose eight *Populus NAC* genes for characterization and high resolution expression analyses using Real-Time PCR. *XND1*, a xylem-associated gene with no clear paralogs in *Arabidopsis* (Zhao et al., 2005), has four orthologs in poplar. Due to the identification of the *XND1* orthologs in *Populus* and the severe vascular-related phenotypes observed in *Arabidopsis XND1* overexpressors (Zhao et al., 2008), we misexpressed *XND1* in *Populus* to investigate the pathways of vascular differentiation in a tree. To further study the function of the selected vascular-associated *Populus NAC* genes, we subjected WT plants to a bending treatment to observe changes in expression coupled with the formation of reaction wood.

3.2 Materials and Methods

3.2.1 Overview of cloning and transformation

Amplification and cloning was accomplished as outlined in the previous chapter. The coding regions of target genes were amplified from cDNA generated by reverse transcriptase (RT-PCR) from extracted *Populus* RNA. The binary vector, pFGC5941, was used in all constructs. For *PopNAC154* constructs in *Populus*, it was necessary to transfer the *35S* promoter, coding region and terminator to another binary vector,

pBINPLUS, which confers kanamycin resistance, as selection of transgenic poplar using basta was problematic (van Engelen et al., 1995). Transformation of the assembled constructs was accomplished by insertion of recombinant plasmid DNA into *Agrobacterium tumefaciens* (*Agrobacterium*) strain AGL1. *Pro$_{35S}$:PopNAC122* was transformed via AGL1 into *Arabidopsis* for phenotypic characterization.

Transformation of poplar tissue was carried out as in Filichkin et al. (2006). Widely used poplar clone 717-1B (*Populus alba x P. tremula*) (referred to as 717, control, WT) was used for transformations. *Agrobacterium* strain AGL1 was used in all *Populus* transformations. Regeneration and propagation of transgenics following transformation was accomplished using the protocol described in Meilan and Ma (2006).

3.2.1.1 Constructs

Pro$_{35S}$:XND1

This gain-of-function construct was obtained from Zhao et al. (2008) and transformed into AGL1 *Agrobacterium* for transformation into *Populus*.

Pro$_{35S}$:PopNAC154

The coding region for *PopNAC154* was amplified from *Populus* stem cDNA using a sense *Xho* I linker primer, *PopNAC154-S*, and an *Eco*R V linker primer, *PopNAC154-3* (Appendix Table I). The resulting PCR product was cloned into the pGEM vector. The sequence of the coding region was verified and digested out of pGEM with *Xho* I/*Swa* I for ligation into the binary vector, pFGC5941, previously digested with *Xho* I/*Sma* I. This resulting vector was used to transform AGL1.

Pro$_{35S}$:PopNAC154-SRDX

The coding region for *PopNAC154* was amplified from the overexpression construct to ensure sequence identity using a sense *Xho I* linker primer, *PopNAC154-S*, and a downstream antisense *Swa* I linker primer, *PopNAC154-AS* (Appendix Table I). *PopNAC154* was digested from pGEM with *Sph* I/ *Swa* I and ligated into pGEM-*SRDX*,

previously digested with *Sma* I/*Sph* I. The *PopNAC154-SRDX* fragment was digested from pGEM with *Xho* I/*Swa* I and ligated into the pFGC5941 vector previously digested with *Xho* I/*Sma* I. The resulting vector was used to transform AGL1.

Pro$_{35S}$*:PopNAC154* and *Pro*$_{35S}$*:PopNAC154-SRDX* into pBINPLUS

Due to the extended time required to obtain transformants using BASTA as selection in tissue culture, the constructs containing *PopNAC154* were modified to confer kanamycin selection. The coding region of *PopNAC154* both with the stop codon and with fusion to the repressor domain was digested from the pFGC5941 vector with *EcoR* I and *Hind* III and subsequently ligated into pBINPLUS, previously digested with *EcoR* I and *Hind* III. The *Pro*$_{35S}$ and OCS terminator were excised with the insert from pFGC5941 for ligation into the multiple cloning site in pBINPLUS.

Pro$_{35s}$*:PopNAC122* and *Pro*$_{35s}$*:PopNAC129* into pFGC5941

The coding region of *PopNAC122* was amplified by PCR from stem cDNA of *Populus alba* using a sense *Xho* I linker primer, *Pa122-S*, and a downstream antisense *EcoR* V linker primer, *Pa122-AS* (Appendix Table I). The PCR product was cloned into the pGEM shuttle vector for sequence verification. pFGC5941, previously digested with *Xho* I/*Sma* I, was ligated with the *PopNAC122* fragment digested from pGEM with *Xho* I/*EcoR* V. The coding region of *PopNAC129* was amplified from the *Populus alba* stem cDNA using the same procedure with a sense *Xho* I linker primer, *NAC129P1*, and an antisense *EcoR* V linker primer, *NAC129P4* (Appendix Table I). The constructs, *Pro*$_{35S}$*:PopNAC122* and *Pro*$_{35s}$*:PopNAC129*, were transformed in AGL1 for *Arabidopsis* transformation.

3.2.1.2 Phylogenetic Analysis

Sequences for *Arabidopsis* were obtained from The *Arabidopsis* Information Resource (TAIR, http://www.arabidopsis.org/). *Populus trichocarpa* sequences were acquired from the Joint Genome Institute *Populus trichocarpa* v1.1 (http://genome.jgi-psf.org/Poptr1_1/Poptr1_1.home.html). Genes from *Vitis vinifera* and *Oryza sativa* were obtained through a GenBank BLAST search (http://blast.ncbi.nlm.nih.gov/Blast.cgi).

Sequence alignment was produced using MUSCLE (http://www.ebi.ac.uk/Tools/muscle/index.html). Phylogenetic analysis was performed using the neighbor-joining tree method in the Mega 4.0.2 computer program (http://www.megasoftware.net/). 1000 bootstrapped data sets were used to infer consensus trees with estimates of statistical confidence.

3.2.2 Analysis of *Populus NAC* Expression

3.2.2.1 Tissue Collection

In stem sections undergoing secondary growth, we collected xylem and PC scrapings from plants grown in greenhouse conditions with a 16h/8h day/night photoperiod at 20 to 22˚C. Xylem and PC sample collection was performed as described in Gray-Mitsumune et al. (2004). In harvesting the tissue for the broad tissue and gradient surveys, the bark was peeled back, revealing the PC on the inner side of the bark. Three to six cell layers from the bark is the PC. The wood side is the developing xylem undergoing secondary wall thickening (Gray-Mitsumune et al., 2004). Both regions were scraped separately into liquid nitrogen and stored at -80˚C. For the whole-bark sample, the PC was not scraped, instead the bark was left intact for RNA extraction. The shoot tip was isolated by removing all recognizable leaves longer than one millimeter from the apical meristem. Leaves were collected from below the apex. Leaf Plastochron Index 1 (LPI 1) refers to the first leaf with a lamina larger than 2 cm (Larson and Isebrands, 1971). The node at LPI 1 is designated as node one with the internodal region below referred to as internode one. For the developmental gradient collection, hand sections from each internode were examined to determine the approximate stage of development. Internodes were pooled according to developmental stage. Internodes two to three represent primary growth, internodes four to seven are indicative of transitional growth and internodes eight to ten correspond to secondary growth. All *Populus* tissues were collected from 717-1B plants with the exception of the floral bud samples which were collected from a naturally grown *Populus alba* clone.

Tension Wood Collection

To induce the production of tension wood, approximately 120 cm-tall control greenhouse plants were bent and tethered by tying each tree at around the 5th internode to the bench creating an angle of about 45˚ and securing the stem to a stake at the 20th internode. For collection of tension and opposite wood, xylem and PC samples from the upper and lower sides of the bent region were collected. As a control, xylem and PC samples were collected from an unbent control tree at the same time.

RNA Extraction

RNA was extracted from *Populus* tissue with modifications to the Qiagen RNeasy mini kit (Qiagen Inc., Valencia, CA) as described in Brunner et al. (2004).

3.2.2.2 3' Rapid Amplification of cDNA Ends (3' RACE)

Due to sequence similarity between the two groups of the *PopNAC*s, 3' RACE was performed for *PopNAC105*, *118*, *122*, *128*, *129*, *154*, *156*, and *157* for Real-Time PCR expression analysis. The 3' untranslated region (3' UTR) generally exhibits a greater degree of divergence enabling the design of gene-specific primers to distinguish between genes exhibiting high sequence homology in the coding region. Using 717-1B Populus cDNA as template, a 100-200 base pair portion of the coding region of select *Populus* genes adjacent to the 3' untranslated region (UTR) was amplified by a gene-specific primer and an adapter primer (*3'RACE adapter*; Appendix Table I) for Real-Time PCR primer design. PCR was run with a Touchdown program (annealing temperature decreased by 0.5˚C each cycle) using Deep Vent$_R$™ DNA polymerase (New England Biolabs, Ipswich, MA). A nested PCR using Taq polymerase (New England Biolabs, Ipswich, MA), a nested gene-specific primer and the adapter primer (Appendix Table I) was run with a 1/20 dilution of the Touchdown PCR product. The resulting DNA fragment was ligated into a shuttle vector, pCR 2.1 (TA Cloning Kit, Invitrogen, Carlsbad, CA), for sequencing. Primers were designed for Real-Time PCR based on the sequence obtained for 3'RACE for each gene.

3.2.2.3 Real-Time PCR

To assess tissue-specific transcript levels of the eight *Populus* genes surveyed, we isolated xylem, bark, PC, leaves, floral buds and shoot apical meristems for quantitative Real Time-PCR (RT-qPCR) analysis. Additional samples were collected in a developmental gradient from LPI 1 to internode ten, consisting of each internode, LPI 1, LPI3, and LPI 6, for RNA extraction. The reactions were run on an Applied Biosystems 7500 Real-Time PCR System (ABI, Foster City, CA) using *Power* SYBR Green PCR Master Mix from ABI. We validated an ubiquitin gene (GenBank CK090058 - *Populus tremula x Populus tremuloides* EST) as an internal control gene for similar expression in the tissues we isolated and to ensure that the gene is a valid reference gene for quantification under our conditions using geNorm software (M < 1.5) (http://medgen.ugent.be/~jvdesomp/genorm/) (Gutierrez et al., 2008). The primers used for ubiquitin amplification were designed from aspen sequence (*aUBQ2-F03*, *aUBQ2-R03*, Appendix Table I). The gene-specific primers used are listed in Appendix Table I. Reactions were run with a total volume of 25 µl and a final primer concentration of 400 nM. The program was modified to increase the primer annealing time from 15 to 20 seconds and to add a dissociation stage. Each sample was run in duplicate within a plate. Each plate was repeated once for a total of four runs per sample. The Ct values were normalized across plates, and 2^(-Delta Delta Ct) analysis was performed according to Livak and Schmittgen (2001).

3.2.3 Analysis of *Populus NAC* Transgenics

3.2.3.1 Tissue Collection

Pro$_{35S}$:XND1 Populus transgenic lines

Due to the stunted growth of the *Pro$_{35S}$:XND1 Populus* plants, most plants could not be transferred from tissue culture to soil. The largest of the plants showing a severe phenotype was transferred in parallel with WT plants into fresh liquid propagation media (Meilan and Ma, 2006) lacking agar to encourage new growth. Plants were grown under a 16h/8h day/night cycle at 20 to 22˚C with gentle shaking until transplanted into soil. Upon acclimation to soil, plants were transferred to larger pots and grown in greenhouse

conditions. Measurements of the *Pro$_{35S}$:XND1* plant and the control plant were taken at 143 days in soil. The stem diameter was measured using digital calipers at two centimeters above the soil surface. Overall height and number of internodes as well as average internode length for both plants was determined. Tissues were collected at 150 days in soil for fixation and embedding. *Pro$_{35S}$:XND1* transgenic stem tissue approximately three internodes from the soil surface was selected for sectioning and examination. Stem tissue from control plants was collected from an area of secondary growth (12th internode) for comparison.

Tissue from several independent events grown in tissue culture was collected for phenotypic characterization. Due to the dwarfed stature of *Pro$_{35S}$:XND1 Populus* events 3B and 14, all of the stem tissue was collected for fixation. Stem tissue for event 11E was excised from the fifth through seventh internode from the media surface. For *Pro$_{35S}$:XND1* line 8 and the control, stem tissue was collected from the second and third internodes above the agar.

RT-qPCR analysis

In order to verify that the *XND1* and *PopNAC154* transgenes were expressed in *Populus* transgenic lines, leaf tissue was collected from several events in tissue culture. One or two small leaves from below the shoot tip were excised for RNA extraction and cDNA synthesis. Primers specific to the *XND1* coding region (*XND1q-Fwd*) and OCS Terminator (*OCSTermq-Rev*) were designed for expression analysis of *XND1* (Appendix Table I). Samples were run in quadruplicate on a single plate with ubiquitin as the reference gene. For *PopNAC154* expression, primers specific to the OCS terminator were designed for RT-qPCR to distinguish transgene expression from expression of the endogenous gene (*OCSF*, *OCS102R*, Appendix Table I). Samples were run in triplicate simultaneously with the internal control gene, ubiquitin.

3.2.3.2 Fixation, embedding and sectioning

Fixation buffers were prepared as in Thornton and Talbot (2006) with a 2% paraformaldehyde/0.5% glutaraldehyde in 10 mM sodium phosphate buffer. Samples

were infiltrated under vacuum at room temperature for one hour followed by one hour of vacuum infiltration on ice. Exceptions to the protocol include washing with 10 mM sodium phosphate buffer and dehydrating with 70% and 90% ethanol, instead of 75 and 95%. Each dehydration step was performed twice for 10 minutes with the exception of the 100% ethanol, which was repeated three times. Samples were subjected to overnight incubation at room temperature with shaking in a 1:1 solution of 100% ethanol and LR White resin (London Resin Company, Ltd., Reading, Berkshire, England). The 1:1 solution was replaced with 100% LR White resin, and samples were incubated overnight at room temperature with shaking. Samples were transferred to 100% LR White resin in gelatin capsules (Electron Microscopy Services, Hatfield, PA) for incubation overnight at 50˚C to let the plastic harden. For sectioning, samples were affixed to a mounting cylinder (Ted Pella, Inc., Redding, CA) with Quick Bond glue (Electron Microscopy Services, Hatfield, PA). Samples were sectioned with glass knives cut at a 45˚ angle on a Sorvall MT2B ultramicrotome.

3.2.3.3 Microscopy

Samples were stained with Toluidine blue/boric acid (0.05% w/v) for one minute. Images were captured under brightfield and fluorescence optics using a Zeiss Axioimager.A1 (EXFO X-Cite Series 120 fluorescent lamp) and under polarized light with a Zeiss Axioscope 40 microscope (Carl Zeiss, Inc., http://www.zeiss.com/). For the *Pro$_{35S}$:XND1* and WT stem sections, rays, vessels and xylem cells were quantified for comparison. A xylem file was defined as a continuous line of cells extending from cambium to pith. Xylem cells and vessels in ten files were counted for both transgenic and WT. A xylem cell was deemed a vessel if it was twice as wide as a cell in the file in which it resided or in files adjacent to the cell. Vessel frequency was reported as a percentage of the total number of cells counted. Statistical significance for xylem cell quantification was determined using the student's *t*-test. The number of rays in a section of 50 xylem files was quantified and reported as a percentage. A ray was defined as having lengthened, narrow cells containing living organelles (Esau, 1965). In the WT and transgenic steles, the radial dimension of the xylem was measured and its proportional contribution to the

total stem radius was calculated. Average cell size was calculated by dividing the radial dimension of the xylem by the average number of cells per file.

3.3 Results

Expression of *AtXND1 Populus* orthologs

XND1 does not cluster phylogenetically or have apparent redundancy with any other *Arabidopsis NAC* genes (Ooka et al., 2003; Zhao et al., 2008). However, *XND1* orthologs are apparent in other annotated genomes. For example, Ooka et al. (2003) noted one *XND1* ortholog in rice, while another was found in a recent genome annotation (http://www.tigr.org/tdb/e2k1/osa1/index.shtml), and at least two *XND1* orthologs are present in the Grape (*Vitis vinifera*) genome. Based on searches of the poplar genome sequence database (http://genome.jgi-psf.org/Poptr_1.home.html) and phylogenetic analyses, four *Populus trichocarpa* genes cluster with *XND1* (Fig. 2a). Each of the four *Populus NAC*s exhibited a distinct expression patterns as indicated by initial microarray data and revealed in more detail by RT-qPCR. For the RT-qPCR experiments, *NAC* gene expression across a developmental leaf and stem (node and internode) gradient was evaluated, and stems with extensive secondary growth were further dissected for analysis of xylem, PC and bark gene expression (Fig. 2b). The highest level of *PopNAC122* expression occurred in secondary tissues of the stem, especially in the PC, where it is expressed 1.3- to 257-fold higher than the other tissues tested. For *PopNAC129*, there was a 400 to 900-fold increase in expression in LPI 1 versus the other leaves as well as a 30-fold increase of expression in the shoot tip compared with internodes two through three. *PopNAC118* was expressed 1.5 to 25-fold higher in nodes compared with all other tissues analyzed. *PopNAC128* exhibited a three- to 475-fold increase in expression in leaf tissues compared with all other tissues not including the shoot tip and floral buds. In vascular tissue, *PopNAC122* and *PopNAC129* were upregulated in the PC compared to xylem while *PopNAC118* was upregulated in bark versus xylem and PC and *PopNAC128* expression was higher in xylem than in PC (Fig. 2b).

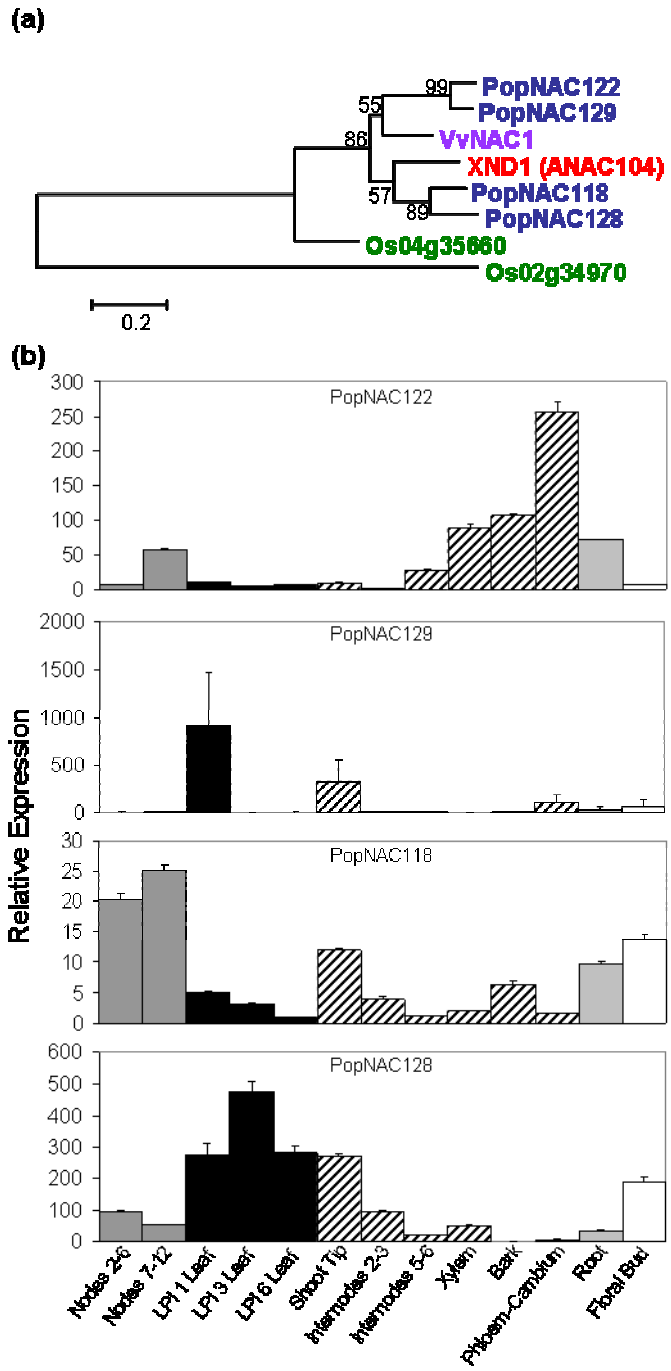

Figure 2. *Populus XND1* orthologs show distinct tissue-type expression patterns. (a) Phylogeny depicting relationship of *XND1* and its orthologs from *Populus*, rice (*Os*) and grapevine (*Vv*). Tree was generated using the neighbor-joining method and bootstrap values of 50% or higher are indicated at the nodes. (b) Tissue samples were collected from greenhouse grown *P. tremula x P. alba* clone 717-1B, except for the floral bud sample that was collected from *P. alba*. Relative transcript quantities were determined by RT-qPCR, normalized to an internal control (*UBQ*), and calibrated to the sample exhibiting lowest relative expression. *PopNAC122* expression was highest in tissues

exhibiting secondary growth whereas its paralog, *PopNAC129*, showed highest expression in primary growth tissues. *PopNAC118* was upregulated in nodes versus all other tissues tested while *PopNAC128* exhibited highest expression in leaf tissues.

Identification and expression of *Populus NAC* genes orthologous to *ANAC073*

To identify additional *NAC* genes that may be regulators of secondary cell wall synthesis outside of the *NST* and *VND* subgroups, we looked for any vascular-associated *NAC* genes that had expression patterns similar to *VND*s and *NST*s. We used the Genevestigator (http://www.genevestigator.ethz.ch/) (Zimmermann et al., 2005) gene correlator function to query the 1122 AtGenExpress chips for expression of all xylem-biased *NAC*s. At4g28500 (*ANAC073*) expression was significantly correlated (R^2 values ranged from 0.65 to 0.89) with expression of *NST1* (At2g46770), *NST2* (At3g61910) and the *NST3* gene (At1g32770). Moreover, *ANAC073* was found by Zhao et al. (2005) to be highly expressed in xylem compared to peripheral tissues of the root-hypocotyl. Although *ANAC073* is coexpressed with the *NST* genes, *ANAC073* shares less than 14% identity with the three NST proteins, which share approximately 60% identity. Four poplar genes cluster with *ANAC073* (Fig. 3a): *PopNAC156*, *PopNAC154*, *PopNAC157*, *PopNAC105*. We surveyed different organs and developmental stages to characterize expression of these four *PopNAC*s. The RT-qPCR results confirmed the initial findings from microarray analyses discussed above (Brunner et al., unpublished), with the expression for each member of the *ANAC073* group being upregulated in xylem compared to PC (Fig. 3b). Specifically, *PopNAC156* and *PopNAC154* exhibited 28 to 33 times higher expression in xylem versus PC whereas *PopNAC157* and *PopNAC105* were upregulated 1.3- to three-fold in xylem compared with PC. In contrast to the *XND1* co-orthologs, the *ANAC073* co-orthologs exhibit a very similar expression pattern in the tissue survey. In each expression profile, there is a steady increase in expression from the shoot tip to the region of secondary growth (Fig. 3b).

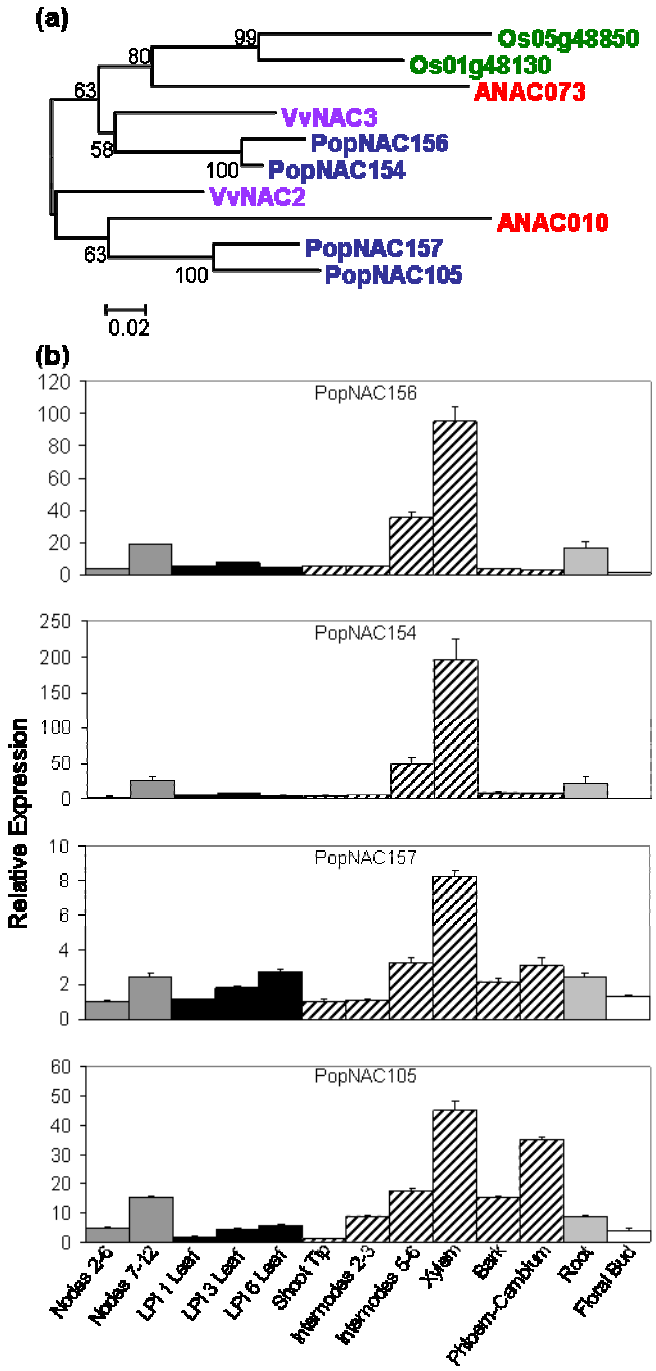

Figure 3. RT-qPCR results from *ANAC073 Populus* orthologs demonstrate similar xylem-specific expression patterns.
(a) Phylogeny showing the relationship of *ANAC073* and its Populus orthologs with rice (*Os*) and grapevine (*Vv*). Tree was generated using the neighbor-joining method and bootstrap values of 50% or higher are indicated at the nodes. (b) Graph showing tissue- and organ-specific expression of *PopNAC156*, *PopNAC154*, *PopNAC157* and *PopNAC105*. Tissue samples were collected from greenhouse grown *P. tremula x P. alba* clone 717-1B, except for the floral bud sample that was collected from *P. alba*. Relative

transcript quantities were determined by RT-qPCR, normalized to an internal control (*UBQ*), and calibrated to the sample exhibiting lowest relative expression. For the *ANAC073* orthologs, relative expression was highest in xylem compared with all other tissues. Expression values increased for all four genes with progression down the stem (i.e. with increasing age of tissue).

Expression of *Populus NAC*s across a developmental gradient

Based on our findings from the organ and vascular tissue survey shown in Figure 2, we decided to perform a higher resolution analysis of changes in gene expression associated with maturation of leaves and development of secondary tissues in stems. Similar to what was observed in the broader tissue survey, four distinct expression patterns were exhibited by the *XND1* subgroup co-orthologs (Fig. 4a). In the stem gradient, *PopNAC122* shows six-fold higher expression in internodes eight to ten compared with internodes two to three reflecting the upregulation in secondary growth observed in the tissue survey results. *PopNAC122* expression is two times higher in the PC than in xylem. Expression of *PopNAC129* is highest in internodes four to five, with a 1.5 to three-fold upregulation compared to the other internodal regions analyzed. In vascular tissues, *PopNAC129* expression is 26 to 27 times higher in the PC and bark compared with xylem. In the stem, *PopNAC118* is most strongly expressed in primary growth and decreases two- to four-fold as stem age increases. Transcript levels for *PopNAC118* were very similar in the PC and xylem. The leaf-associated expression of *PopNAC128* (Fig. 2) was further resolved in Figure 4 and shown to peak in developing leaves with a four-fold increase relative to young and mature leaves. *PopNAC128* expression in xylem is 14 times higher than in the PC, although the level of expression in leaves is five to 1728 times higher than in all other tissues tested (Fig. 4a).

The RT-qPCR developmental gradient analysis for the *ANAC073* subgroup support the results from the broad tissue survey, i.e. that the four *Populus NAC*s exhibit nearly identical relative expression patterns (Fig. 4b). All four genes show a steady increase in expression from internodes two through three to the eight through ten internodal region. Expression of the *ANAC073* co-orthologs is six to 149 times higher in xylem compared with the PC. In leaf tissues, the expression level increases from LPI 1 to LPI 3 for all four genes (Fig. 4b).

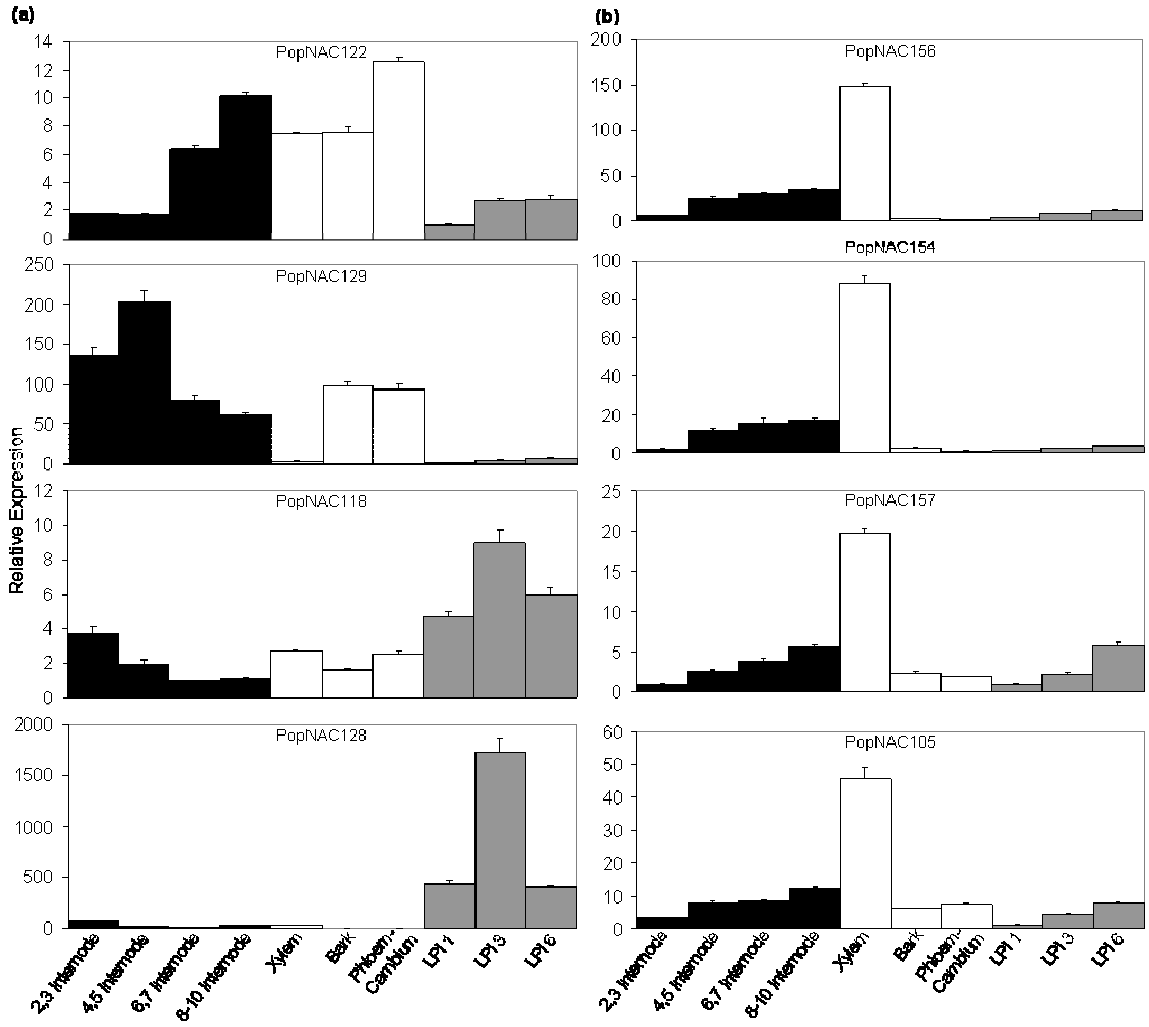

Figure 4. RT-qPCR results from high resolution analysis of expression along a developmental gradient in *Populus*.
Tissue samples were collected from greenhouse grown *P. tremula x P. alba* clone 717-1B. Relative transcript quantities were determined by RT-qPCR, normalized to an internal control (*UBQ*), and calibrated to the sample exhibiting lowest relative expression. (a) *XND1* orthologs exhibit differences in expression patterns even among paralogs. *PopNAC122* is upregulated in tissues developing secondary growth. Expression of *PopNAC129* shows upregulation in primary and transition growth. Paralogs *PopNAC118* and *PopNAC128* are upregulated in primary vascular tissues as well as leaves compared with other tissues surveyed. (b) *ANAC073* orthologs display xylem- and secondary growth-specific expression with nearly identical patterns. All of the genes show an increase in relative expression from shoot tip to secondary growth and exhibit an increase in expression in xylem compared with PC.

Expression of *Populus NAC*s in tension and opposite wood in response to bending stress

In response to the bending treatment, the four members of the *XND1* group exhibited distinct expression patterns. All four genes were upregulated in opposite xylem compared to tension xylem to varying degrees (Fig. 5a). In addition, three of the four genes were upregulated in opposite xylem compared to vertical xylem. In contrast, only *PopNAC128* and *PopNAC118* were upregulated in opposite PC compared to tension and vertical PC. *PopNAC122* and *PopNAC129* were upregulated 1.2 to three-fold in vertical PC versus tension or opposite PC (Fig. 5a).

In contrast to the results for the *XND1 Populus* orthologs, the expression of the *ANAC073* subgroup members show little change in response to the bending treatment. There were a few slight differences in the xylem samples, but little to no variation in expression levels is seen across PC samples (Fig. 5b). For *PopNAC156 and PopNAC105*, a 1.2- to two-fold decrease in expression is induced in the tension and opposite xylem samples versus vertical xylem (Fig. 5b). *PopNAC154* and *PopNAC157* show a 1.4- to 1.5-fold decrease in tension xylem compared to vertical and opposite xylem (Fig. 5b).

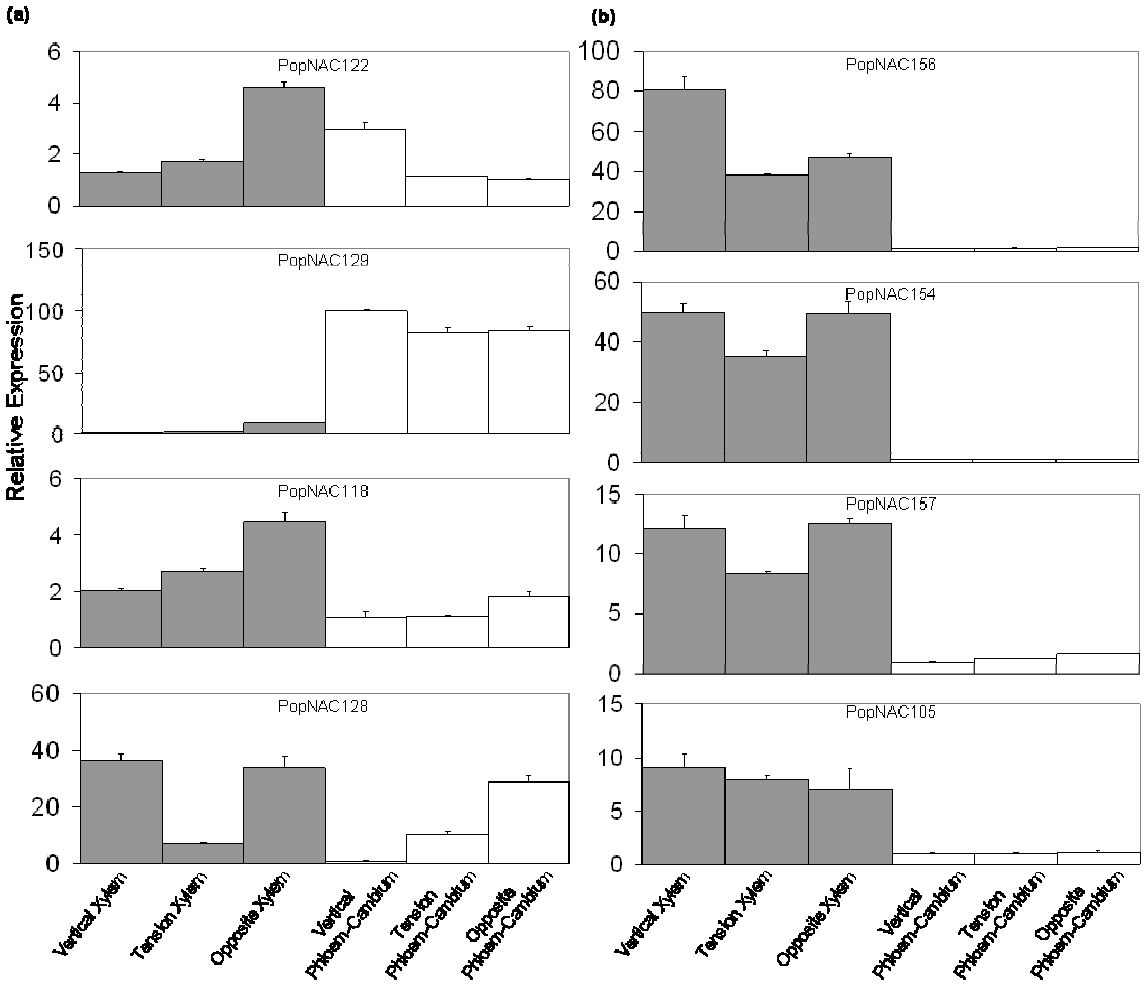

Figure 5. Expression of *Populus NAC*s in tension and opposite wood in response to bending stress.

Tissue samples were collected from greenhouse grown *P. tremula x P. alba* clone 717-1B, both treated (bent) and untreated (vertical). Individuals were bent for a period of one week. Relative transcript quantities were determined by RT-qPCR, normalized to an internal control (*UBQ*), and calibrated to the sample exhibiting lowest relative expression. (a) The expression of *XND1* orthologs in both xylem and PC is altered in response to the bending treatment. All four genes were upregulated in opposite xylem compared with tension xylem. Three of the four genes were upregulated in opposite xylem compared to vertical (unbent) xylem. *PopNAC118* and *PopNAC128* were upregulated in opposite PC compared with vertical and tension PC whereas *PopNAC122* and *PopNAC129* were upregulated in vertical PC versus tension and opposite PC. (b) *ANAC073* ortholog expression in response to bending exhibit slight changes in xylem, but little or no differences in PC. *PopNAC154* and *PopNAC157* showed a downregulation in tension xylem compared to opposite xylem, which remained unchanged compared to vertical xylem. *PopNAC156* and *PopNAC105* exhibit a decrease in both tension and opposite xylem relative to vertical xylem.

Expression of *XND1* in *Populus* tissue culture plants

Since *XND1* expression cassettes were available in advance of those for expression of the poplar *XND1* orthologs, we investigated the effect of overexpressing *XND1* in *Populus,* as a preliminary test of possible roles for the poplar *XND1* orthologs. Nineteen independent transgenic events overexpressing *XND1* were produced. Of the nineteen events, eleven exhibited phenotypes differing from WT. These phenotypes ranged from moderately stunted and dark green compared to controls to severely stunted plants exhibiting absence of phloem fibers, changes in vessel frequency and size and a significant reduction in growth and development of secondary vasculature. For some of the most severely affected plants, the original shoot would either cease development or die, but numerous healthy shoots would arise from the roots, termed "root suckering," a common occurrence in aspen (Wan et al., 2006). The remaining nine events looked identical to WT. Figure 6 shows four of the events exhibiting a stunted growth phenotype (a-d). Cross-sections of the stems from individual plants from each independent event are shown (Fig. 6f-i) for comparison with a WT plant of similar size but is two to 8.5 months younger than the transgenics shown (Fig. 6e,j). Event 11, which is the oldest of the transgenics, was the most similar to WT (Fig. 6f). The control plants in tissue culture generally reach the tops of the boxes within 1.5 to two months. All of the *Pro_{35S}:XND1* plants have developing xylem tissue, but none of the cross-sections show any developing phloem fibers, which can be clearly seen in the younger control plant (compare Fig. 6f-i to j). Note that xylem vessels in the transgenics are not as large or as numerous as those seen in the WT plant (compare Fig. 6f-i to j). The relative level of *XND1* expression as determined by RT-qPCR was highest in events 8, 11E and 14 (Appendix Table X). Due to the severe phenotype observed in event 14, an individual transgenic plant was chosen for further analysis and characterization.

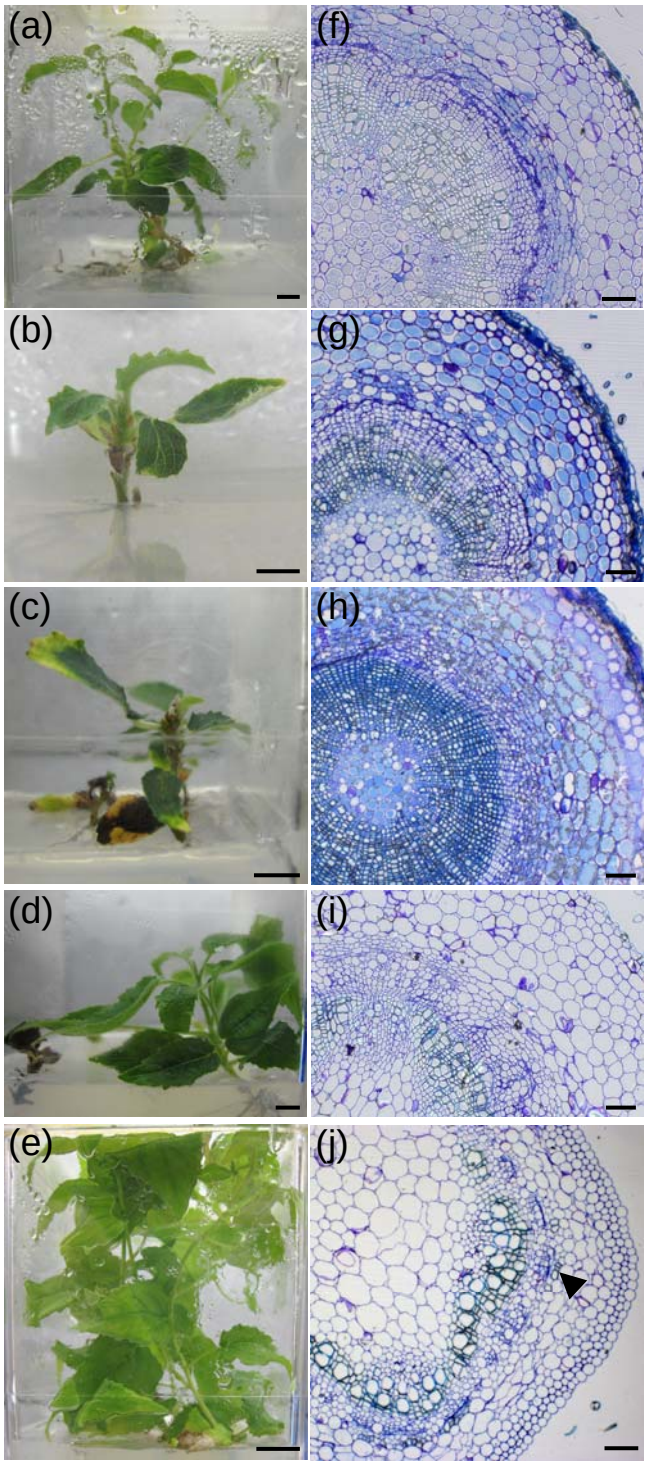

Figure 6. Misexpression of *XND1* in *Populus* induces severe stunting associated with an absence of phloem fibers and varying degrees of secondary growth inhibition.
(a-d) Images of *Pro*$_{35S}$*:XND1 Populus* events in tissue culture exhibiting a stunted phenotype (arranged oldest to youngest from top to bottom). (e) Image of wild-type *Populus* plant in tissue culture that is two to 8.5 months younger than the transgenics

shown in panels a-d. (f-i) Brightfield micrographs of stem cross-sections of *Pro$_{35S}$:XND1 Populus* events stained with Toluidine Blue from panels a-d showing varying degrees of abnormal vascular differentiation featuring a lack of phloem fibers, smaller cell size and number in vascular tissues and reduced vessel density. (j) Cross-section of wild-type *Populus* (from panel e) captured under brightfield optics following Toluidine Blue staining. Normal phloem fiber development is indicated by arrowhead in j. Bars = 0.5 cm in (a)-(d); 1 cm in (e); 0.05 mm in (f) for (g)-(j).

Pro$_{35S}$:XND1 Populus plants were severely stunted similar to *Pro$_{35S}$:XND1 Arabidopsis* plants

Transgenics overexpressing *XND1* display a phenotype similar to that seen in *Arabidopsis* plants overexpressing *XND1*. One transgenic *Pro$_{35S}$:XND1* plant (*Pro$_{35S}$:XND1.14*) was transferred in parallel with a control plant from tissue culture to soil. The transgenic plant was extremely stunted compared to the WT plant at 129 days in soil (Fig. 7b). After 143 days in soil, the WT plant measured 93.7 cm in height with 44 internodes and a diameter of 7.14 mm while *Pro$_{35S}$:XND1.14* was 10.2 cm in height with 17 internodes and a diameter of 1.93 mm. Average internode length for *Pro$_{35S}$:XND1.14* was 0.6 cm while the control was 2.1 cm. Figure 7a shows a cross-section of the lower stem of *Pro$_{35S}$:XND1.14* and Figure 7d shows a cross-section of the 12th internode of a WT plant with both images taken at the same magnification for comparison. There are almost no phloem fibers in the transgenic plant while several large bundles of phloem fibers are visible in the control (compare Fig. 7c,d). Also reduced are rays, which are present at a 10% lower rate of occurrence in the transgenic plant compared with the WT plant. Of the ten files examined, five of the files in *Pro$_{35S}$:XND1.14* had no vessels whereas the WT had one to six vessels in each file. Xylem accounts for only 52.9% of the stem radius in *Pro$_{35S}$:XND1.14* compared with 71.6% in the control, a reduction of 18.7% due to *XND1* overexpression. Reductions in cell size (Fig. 7a,c; Appendix Table VIII) and cell number (Appendix Table VIII) both contribute to the smaller xylem area. Despite the notable changes in cell size, cell fate and cell number, xylem cells in *Pro$_{35S}$:XND1.14* exhibited apparently normal lignification, based on autofluorescence (Fig. 7e,f), and similar birefringence emitted from the lignified cells in the xylem of transgenic and WT plants (Fig. 7g,h).

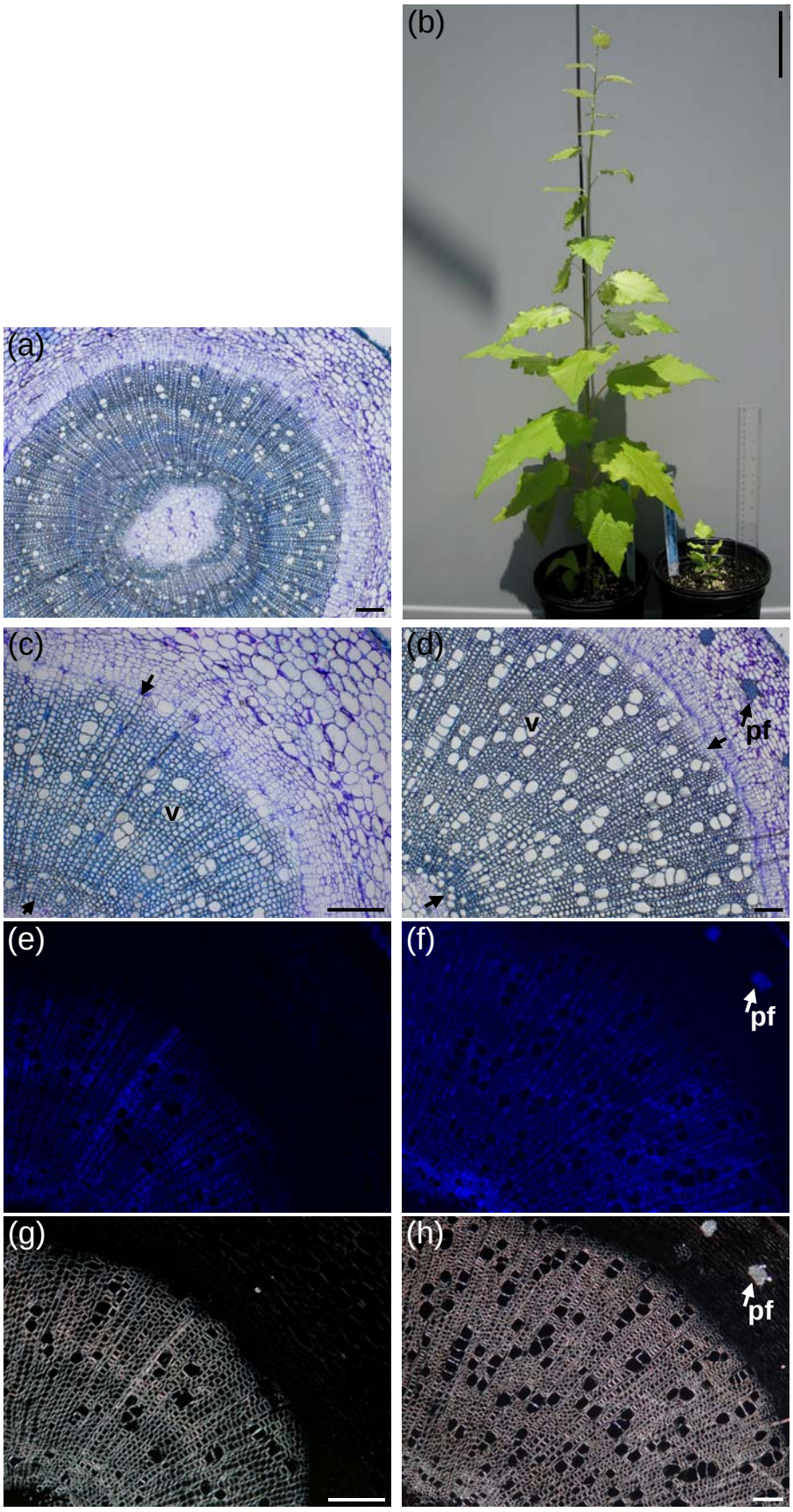
(a)
(b)
(c)
v
(d)
v
pf
(e)
(f)
pf
(g)
(h)
pf

Figure 7. Overexpression of *XND1* in *Populus* led to a reduction in the rate of cell division and cell size in xylem, decreased production of vessels and rays in xylem and the near complete absence of phloem fibers.
Shown are *Pro$_{35S}$:XND1* dwarf (*Pro$_{35S}$:XND1.14*) (a, b - plant on right, c, e, g) and wild-type (b – plant on left, d, f, h) plant. (a) Brightfield image of cross-section of the lower stem in *Pro$_{35S}$:XND1.14* stained with Toluidine Blue taken at same magnification as the wild-type in panel d (to emphasize reduced cell size in *Pro$_{35S}$:XND1.14* compared to wild-type xylem). (b) Image of wild-type (left) and the severely stunted *Pro$_{35S}$:XND1* transgenic (right) after 129 days in soil. Both control and transgenic were processed in parallel from tissue culture to soil. (c) *Pro$_{35S}$:XND1.14* transgenic stem cross-section stained with Toluidine Blue showing absence of phloem fibers and a reduction in vessel (v) frequency versus the control. The number of xylem cells per file was significantly different from the wild-type ($p<0.0001$). A reduction in the number of rays (r, arrows indicating ends of an individual) compared with wild-type was also observed. (d) Brightfield image of wild-type cross-section from the 12th internode stained with Toluidine Blue showing clear phloem fiber bundles (pf, arrow). Rays (r, arrows at ends) and vessels (v) are indicated. (e) Image of *Pro$_{35S}$:XND1.14* cross-section emitting autofluorescence from lignified cells in xylem. (f) Wild-type cross section showing autofluorescence from lignified cells in the xylem and phloem fibers (pf, arrow). (g) Polarized image of *Pro$_{35S}$:XND1.14* transgenic cross-section exhibiting birefringence in lignified xylem cells. (h) Image under polarized optics of wild-type cross-section showing birefringence in xylem cells and phloem fibers (pf, arrow) with lignification. Bars = 100 μm in (a), (g), (h); the bar in (c) for (e) = 100 μm; the bar in (d) for (f) = 100 μm; 10 cm in (b).

Pro$_{35S}$:PopNAC122 and *Pro$_{35S}$:PopNAC129 Arabidopsis* plants exhibit xylem discontinuity and stunted growth

Pro$_{35S}$:PopNAC122 Arabidopsis plants have a phenotype similar to that reported for *Pro$_{35S}$:XND1 Arabidopsis* plants (Zhao et al., 2008). At four weeks old, T_2 plants are dark green and stunted (Fig. 8a) compared with the vector-only control plants (Fig. 8b). In addition to the dwarfed stature, xylem development in the roots of the *PopNAC122*-overexpressing plants is blocked or delayed and lacks protoxylem poles (Fig. 8c), while vector-only control plants undergo normal xylem development consisting of two protoxylem poles flanking three or four files of metaxylem vessels (Fig. 8d). The repression of xylem vessel differentiation is illustrated in Figure 1 where mature vessel elements in the zone of differentiation are detectable in controls within 1 mm from the root tip (panel f), while a typical *Pro$_{35S}$:PopNAC122* plant has no detectable xylem within 10 mm from the root tip (e). Interestingly, *Pro$_{35S}$:PopNAC122* plants do initiate lateral roots (Fig. 8e,g); however, discontinuity between the xylem in the lateral roots and

that in the primary root was commonly observed (Fig. 8g) in transgenics compared to vector-only control plants (Fig. 8h).

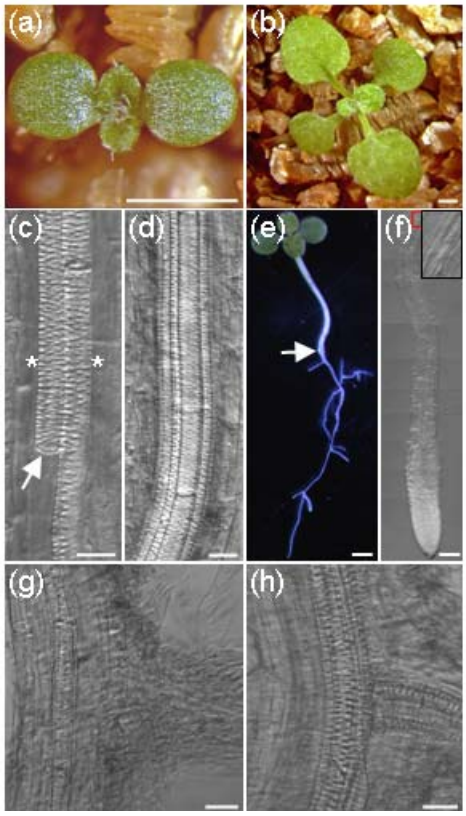

Figure 8. Expression of *PopNAC122* in *Arabidopsis* results in stunted plants exhibiting xylem discontinuity as well as an absence of protoxylem poles.
Shown are *Pro$_{35S}$:PopNAC122* dwarf (a, c, e, g) and vector-only control (b, d, f, h). (a) Four-week-old T_2 *Pro$_{35S}$:PopNAC122* plants are dark-green and stunted compared with control plants such as the one seen in panel (b). (c) Mature metaxylem elements are discontinuous (arrow) in the root-hypocotyl of the *Pro$_{35S}$:PopNAC122* transgenics. Transgenics lack protoxylem poles (*). (d) The normal arrangement of a central metaxylem file flanked by narrower metaxylem files with protoxylem poles to the outside is seen in the root-hypocotyl of the controls. (e) Image of a *Pro$_{35S}$:PopNAC122* dwarf with an arrow at the point of discontinuity, 10 mm from the root tip. (f) Control root tip showing the point of discontinuity (red bracket), 1 mm from the root tip (enlarged in inset). (g) Lateral roots formed in the *Pro$_{35S}$:PopNAC122* transgenics (panel e), but failed to establish normal xylem continuity between the main root and lateral root as seen in the control (h). Bars = 1.25 mm for (a) and (b); 10 µm for (c), (d), (f), (g), (h); 1 mm in (e).

Pro$_{35S}$:PopNAC154 transgenic lines

Fifteen independent transgenic events were regenerated from transformations with *Pro$_{35S}$:PopNAC154*. No visible deviation from the WT phenotype was seen in the tissue culture plants with confirmed transgene expression. cDNA from ten *PopNAC154*-overexpressing individuals was isolated to quantify the level of transgene expression in each independent event. Three of the ten events exhibited expression levels four to 40 times higher than the other events (Fig. 9). Of the seven events with lower expression levels, the expression of the *PopNAC154* transgene in five of the events was upregulated three to ten times higher than in the remaining two events (Fig. 9).

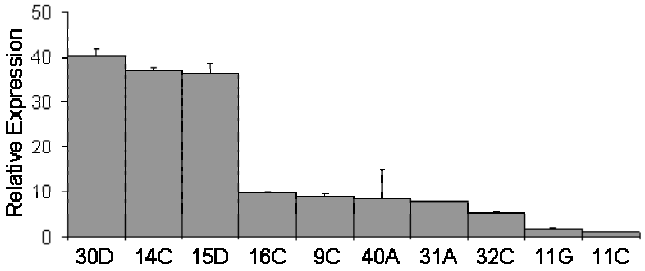

Figure 9. Expression level of the *Pro$_{35S}$:PopNAC154* transgene in independent poplar transgenic events analyzed by RT-qPCR.

Shoot regeneration in *Pro$_{35S}$:PopNAC154-SRDX* transformants

Control tissue was transformed with the *Pro$_{35S}$:PopNAC154-SRDX* construct. Explants resulting from transformation formed shoots, but were unable to initiate root formation. Shoots were screened for transgene presence; however, no events expressing the transgene were recovered from transformations with the *Pro$_{35S}$:PopNAC154-SRDX* construct. Similar to our results with poplar, two independent transformations of *Arabidopsis* plants for expression of *ANAC073-SRDX* (*ANAC073* is a *PopNAC154* ortholog) also failed to yield any transgenic plants, while overexpression of *ANAC073* yielded only transgenics with WT appearance.

Discussion

XND1 Populus orthologs exhibit distinct patterns of expression across tissue types and along a developmental gradient

Taking into account the more complex anatomy and seasonal nature of the secondary vasculature of a tree relative to *Arabidopsis*, it seems logical that roles performed in xylem by one gene in *Arabidopsis* may require the activities of several genes in *Populus*. Their distinct expression patterns suggest the possibility that the four *XND1* orthologs control different aspects of vascular development. Elevated expression in the PC and in regions of secondary growth suggests that *PopNAC122* is possibly involved in secondary growth in PC such as in the development of phloem fibers (Figs. 2b and 4a). Since it is also highly expressed in xylem tissues, *PopNAC122* might be involved in the development of secondary growth in xylem. *PopNAC129*, a paralog of *PopNAC122*, shows higher expression in primary-to-transition stages of stem vascular development. With highest expression in internodes four to five and PC, *PopNAC129* might be involved in the transition from primary to secondary growth in PC. *PopNAC118* is most highly expressed in the nodes suggesting a role in cambial development or perhaps a more general role in regulation of cell fate. *PopNAC128* shows strong expression in the leaf tissues, with expression five to 1700 times higher in leaves compared with all other samples. The elevation of expression in leaf tissue suggests that *PopNAC128* might regulate vascular tissue formation or differentiation in leaves (Figs. 2b and 4a). However, in situ hybridization results show expression associated with mesophyll cells in developing leaves supporting a role for at least one *XND1* ortholog in non-vascular cell types (Brunner et al., unpublished).

The expression patterns of the *XND1* orthologs along the stem gradient seem to complement each other in that each gene appears to be most active during a different stage of development. *PopNAC118* and *PopNAC128* exhibit a similar pattern in which the highest expression occurs in the shoot tip or primary growth region and decreases with the progression down the stem (Fig. 4a). The expression of *PopNAC129* increases

two-fold from internodes two to three where it reaches a peak at internodes four to five and then decreases three-fold down the stem. In contrast, *PopNAC122* expression is lower in internodes two to five and exhibits a four- to six-fold increase at internodes six to ten. Given that the expression for each of the *XND1* orthologs is peaking at a different developmental stage, the genes may be involved in the same processes but in separate tissues or at different times during development. All four genes may be interacting to implement the seasonal changes in development involved in dormancy and cessation of growth as well as initiation of growth, proliferation and expansion. It would be interesting to study the changes in expression for the *XND1* orthologs by inducing dormancy and growth initiation.

Expression patterns of *ANAC073 Populus* orthologs are nearly identical in a developmental gradient

In contrast to the *XND1* orthologs, the *ANAC073* group of genes exhibit very similar expression patterns, especially among the two paralogous pairs. Each of the four genes is more highly expressed in xylem than in any other tissue surveyed suggesting that they are xylem-specific and may interact to regulate xylem formation and differentiation (Figs. 3b and 4b). Expression of the four genes increases with the progression down the stem and is highest in regions of secondary growth (Figs. 3b and 4b). Based on the expression data, the genes are possibly involved in the regulation and control of secondary cell wall synthesis in xylem. The intricate process of wood formation in a tree requires a complex network of interactions which may explain the need for four genes with similar expression profiles. It is possible that each of the genes is activated during a different stage of development. At this level of investigation, it is unclear what roles these genes play despite their association with vascular tissues.

In situ hybridization using probes specific to each gene would provide information about tissue-specific expression throughout the plant. Further characterization through the development of RNAi constructs gene-specific silencing would aid in determining their individual roles in vascular tissue development.

Stimulation of reaction wood formation in *Populus* leads to proposed gene-specific functions

In order to obtain more information about the function of the *PopNAC*s, we subjected WT trees to bending stress to potentially alter the expression of these genes. We used RT-qPCR to monitor the changes in gene expression of members in both the *XND1* and *ANAC073 Populus* ortholog groups. The normal progression of secondary wall biosynthesis is altered in the formation of tension (or reaction) wood (Andersson-Gunneras et al., 2006). Tension wood is characterized by an increase in cellulose content at the cost of a reduction in lignin and hemicellulose as well as a reduction in vessel element frequency and size (Andersson-Gunneras et al., 2006). Wu et al. states that an increase in lignin coupled with a decrease in cellulose is seen in the compression-stressed tissues opposite the tension wood (2000). An increase in cambial cell division is observed in tension wood in contrast to opposite wood in which cambial growth is inhibited (Hellgren et al., 2004). Upon comparison of values for relative expression (xylem vs. PC) for the tissue and gradient surveys and expression of vertical (unbent) xylem versus PC, the values were not identical but the patterns and the degree of expression level for xylem versus PC in both groups were similar. For example, *PopNAC122* and *PopNAC129* are upregulated in PC while *PopNAC118* and *PopNAC128* are upregulated in xylem across all three surveys (Fig. 5a).

Varied responses to the gravitational stimulus were seen in the *XND1* group suggesting possible roles in cambial development and secondary wall biosynthesis. *PopNAC122* and *PopNAC129* show a three- to eight-fold increase in expression in opposite xylem and a 1.2- to three-fold downregulation in tension and opposite PC compared with vertical PC (Fig. 5a). The upregulation in opposite xylem suggests that *PopNAC122* and *PopNAC129* are either having a negative effect on cellulose content and cambial cell division or a positive effect on lignification in opposite wood. Expression of the paralogs in treatment-induced PC is decreased implying that the genes might not be involved in changes occurring in tension and opposite PC. Based on their expression patterns in xylem from RT-qPCR, it seems that *PopNAC129* may be affecting cambial cell division whereas *PopNAC122* is presumably controlling secondary growth aspects of development such as

the formation of cellulose or lignin. A two-fold increase in both opposite xylem and PC and elevated expression in tissues involving growth initiation suggest that *PopNAC118* might be involved in the inhibition of cambial growth in opposite wood. *PopNAC128* exhibits a decrease in tension xylem coupled with an increase in expression in both tension and opposite PC. Based on the bending-induced changes in expression and the potential role in cambial initiation from RT-qPCR, *PopNAC128* may also be regulating cambial development. Considering the upregulation of three of the *XND1* orthologs in both tension and opposite xylem compared with vertical xylem, the changes observed in the poplar *XND1* overexpressors such as reduction in cell size/number, overall extent of xylem, and vessel frequency are similar to the vascular modifications induced in tension and opposite wood.

Changes in gene expression for the *ANAC073* orthologs as a result of the bending treatment were subtle and consistent among the four genes in contrast to the distinct patterns observed for the *XND1* group. All four *ANAC073* orthologs exhibit a 1.2- to two-fold decrease in expression in tension xylem (Fig. 5b). *PopNAC156* and *PopNAC105* also show a decrease in opposite xylem. Based on xylem-specific expression implicated by the RT-qPCR results, these four genes are probably coordinating the control of lignification and cellulose formation in xylem. Functional redundancy may be required in *Populus* to mediate the regulation of secondary growth in response to seasonal changes.

XND1 misexpression in _Populus_ resulted in stunted plants lacking phloem fibers and exhibiting a reduction in ray and vessel frequency in xylem

Results from misexpression of *XND1* in *Arabidopsis* show that *XND1* blocks secondary wall synthesis and programmed cell death in xylem (Zhao et al., 2008). In contrast, overexpression of other xylem-specific *NAC* genes involved in secondary growth such as *NST1*, *NST2* (Mitsuda et al., 2005), *VND6* and *VND7* (Kubo et al., 2005) resulted in stimulation of ectopic secondary wall formation. Since *XND1* has four orthologs in *Populus*, we overexpressed *XND1* in *Populus* for further analysis of *XND1* function and to investigate the genetic pathways involved in vascular tissue formation in *Populus*. Two of the *XND1* orthologs are upregulated in PC compared to xylem, *PopNAC122* and

PopNAC129. Given that *XND1* misexpression in *Arabidopsis* leads to repression of secondary wall synthesis in xylem, overexpression of *XND1* in *Populus* may have affected the secondary wall synthesis in phloem fibers reflecting the PC-associated expression we observed for the two *XND1* orthologs. As seen in Figure 7, lignification occurs in the xylem despite the overexpression of *XND1*. Extent of lignification may be different in transgenic versus WT; however, detailed analysis of cell wall composition and electron micrographs may be necessary to detect any discernable differences. Secondary wall synthesis in xylem may be controlled through a different mechanism or set of genes in *Populus* that is not affected by *XND1* misexpression. Although lignification in xylem cells was apparently unaffected by the transgene, the extent and organization of xylem in the stele, number of xylem cells per file and ray and vessel frequency as well as overall growth were influenced by overexpression of *XND1*. The notable differences in cell size and vessel number are easily seen when comparing *Pro$_{35S}$:XND1.14* and wild-type cross-sections at the same magnification (Figure 7a,d). Stunted growth in the transgenics both in tissue culture (Fig. 6) and soil (Fig. 7) may be the consequence of the observed disruptions in vascular tissue function resulting from the vessel- and ray-deficiencies, in addition to the absence of phloem fibers. The four-fold reduction in average internode length suggests that development is arrested in the transgenic in addition to the dwarfed stature. Without efficient transport of nutrients and water, the potential for normal, healthy growth is diminished. Abnormalities in the xylem and phloem of plants exhibiting the dwarf phenotype might also provide an explanation for the death of the shoot tip leading to the "root suckering" observed in the more severe phenotypes. Due to the potential roles of the *XND1 Populus* orthologs in cambial cell development, it is possible that *XND1* may have an effect on cell division and cell fate in *Populus*, which may explain the decrease in the number of xylem cells per file as well as the nearly 20% reduction in the xylem component of the stem radius as compared with the control ratio. If *XND1* is indeed affecting cell fate, that might also explain the decrease in rays and vessels observed in the transgenic. Taking the bending data into account, three of the *XND1* orthologs exhibit a 1.3- to two-fold increase in tension xylem and a two- to eight-fold upregulation in opposite xylem compared with vertical xylem. As tension xylem is characterized by a decrease in vessels and an inhibition of cambial cell

division is indicative of opposite xylem (Andersson-Gunneras et al., 2006), the phenotype we observed for *XND1* overexpressors may reflect the roles of *XND1* orthologs in tension and opposite wood development. The effects observed in the poplar vascular tissues resulting from the overexpression of *XND1* appear to mimic the cell- and tissue-level developmental changes observed in tension and opposite wood in response to a gravitational stimulus. NAC domain proteins are known to form homodimers and heterodimers with other family members in yeast two-hybrid experiments (Xie et al., 2000; Bu et al., 2008; Yamaguchi et al., 2008). Hence, the complex expression patterns exhibited by these four *XND1* orthologs may reflect combinatorial regulation of cell fate in multiple tissues and developmental contexts, and also suggests that *XND1* interacted with its orthologs in transgenic *Populus*.

Pro$_{35S}$:PopNAC122 phenocopies *Pro$_{35S}$:XND1* in *Arabidopsis*

When *PopNAC122*, an *XND1* ortholog, is overexpressed in *Arabidopsis*, the phenotype observed is very similar to the phenotype of the *Pro$_{35S}$:XND1* plants described in Zhao et al. (2008). Both *Pro$_{35S}$:XND1* and *Pro$_{35S}$:PopNAC122 Arabidopsis* plants exhibit severe dwarfing, discontinuous xylem and the absence of protoxylem poles (Fig. 8) (Zhao et al., 2008). Another aspect of xylem discontinuity observed in the transgenics was that observed between the laterals and the main root. The stunted phenotype is possibly caused by the disconnected network of xylem resulting in an inability to effectively transport water long distances and illustrates the difficulty of distinguishing between primary and secondary effects of overexpression experiments. RT-qPCR data shows that *PopNAC122* is highly expressed in PC and increases in regions of secondary growth in *Populus* while *XND1* is highly expressed in *Arabidopsis* xylem (Figs. 2b and 4a) (Kubo et al., 2005; Zhao et al., 2005). Since the role of *PopNAC122* is unknown, the expression of the gene in *Arabidopsis* may be mimicking suppression of xylem differentiation observed in overexpressors of *XND1* perhaps due to the degree of sequence similarity shared between the two genes. *XND1* lacks paralogs in *Arabidopsis* while *Populus* is a more complex, temperate zone tree with four orthologs of *XND1*. Despite its apparent ability to phenocopy the effects of *XND1* overexpression, *PopNAC122* may nevertheless

regulate a developmental process specific to a tree that has no parallel pathway in *Arabidopsis*.

Pro$_{35S}$:PopNAC154 transformants exhibit a WT phenotype in tissue culture

Based on the high expression of *PopNAC154* in xylem observed in the microarray data, we transformed WT plants with a construct for overexpression of *PopNAC154*. Since no phenotype was observed in tissue culture plants exhibiting expression of the transgene, future characterization will involve transgenic plants that have been transferred to soil. Given that *PopNAC154* expression is highest during secondary growth in the stem, studying larger plants exhibiting a greater degree of secondary growth and wood formation will potentially reveal a vascular tissue-related phenotype.

Pro$_{35S}$:PopNAC154-SRDX transgenics were not recovered from transformations

To overcome impending functional redundancy due to the presence of three close homologs of *PopNAC154* in *Populus*, we fused the *PopNAC154* coding region to the SRDX repression domain. The NAC-SRDX fusions have proven to be effective for functional characterization in other studies involving NAC transcription factors with genetic redundancy (Kubo et al., 2005; Mitsuda et al., 2005). No transgenics were regenerated suggesting that the effect of the *PopNAC154-SRDX* fusion prevented shoot and/or root formation. This further suggests that *PopNAC154* and its homologs may therefore play a broader role in regulating plant development, perhaps by regulating cell fate in various tissues and developmental stages.

References

Aida, M., Ishida, T., Fukaki, H., Fujisawa, H., and Tasaka, M. (1997). Genes involved in organ separation in Arabidopsis: an analysis of the cup-shaped cotyledon mutant. Plant Cell 9, 841-857.

Andersson-Gunneras, S., Mellerowicz, E.J., Love, J., Segerman, B., Ohmiya, Y., Coutinho, P.M., Nilsson, P., Henrissat, B., Moritz, T., and Sundberg, B. (2006). Biosynthesis of cellulose-enriched tension wood in Populus: global analysis of transcripts and metabolites identifies biochemical and developmental regulators in secondary wall biosynthesis. Plant J 45, 144-165.

Brunner, A.M., Yakovlev, I.A., and Strauss, S.H. (2004). Validating internal controls for quantitative plant gene expression studies. BMC Plant Biol 4, 14.

Bu, Q., Jiang, H., Li, C.B., Zhai, Q., Zhang, J., Wu, X., Sun, J., Xie, Q., and Li, C. (2008). Role of the Arabidopsis thaliana NAC transcription factors ANAC019 and ANAC055 in regulating jasmonic acid-signaled defense responses. Cell Res 18, 756-767.

Chen, H., Nelson, R.S., and Sherwood, J.L. (1994). Enhanced recovery of transformants of Agrobacterium tumefaciens after freeze-thaw transformation and drug selection. Biotechniques 16, 664-668, 670.

Clough, S.J., and Bent, A.F. (1998). Floral dip: a simplified method for Agrobacterium-mediated transformation of Arabidopsis thaliana. Plant J 16, 735-743.

Cress, W.D., and Triezenberg, S.J. (1991). Critical structural elements of the VP16 transcriptional activation domain. Science 251, 87-90.

DOE. (2005). Industrial Technologies Program, Fiscal Year 2004 Report.

Esau, K. (1965). Plant Anatomy, Ed 2nd. (New York: John Wiley & Sons).

FAO. (2005). State of the World's Forests. In Food and Agriculture, Organization of the United Nations, Rome, Italy.

Filichkin, S.A., Meilan, R., Busov, V.B., Ma, C., Brunner, A.M., and Strauss, S.H. (2006). Alcohol-inducible gene expression in transgenic Populus. Plant Cell Rep 25, 660-667.

Gray-Mitsumune, M., Mellerowicz, E.J., Abe, H., Schrader, J., Winzell, A., Sterky, F., Blomqvist, K., McQueen-Mason, S., Teeri, T.T., and Sundberg, B. (2004). Expansins abundant in secondary xylem belong to subgroup A of the alpha-expansin gene family. Plant Physiol 135, 1552-1564.

Gutierrez, L., Mauriat, M., Guenin, S., Pelloux, J., Lefebvre, J.F., Louvet, R., Rusterucci, C., Moritz, T., Guerineau, F., Bellini, C., and Van Wuytswinkel, O. (2008). The lack of a systematic validation of reference genes: a serious pitfall undervalued in reverse transcription-polymerase chain reaction (RT-PCR) analysis in plants. Plant Biotechnol J 6, 609-618.

Hellgren, J.M., Olofsson, K., and Sundberg, B. (2004). Patterns of auxin distribution during gravitational induction of reaction wood in poplar and pine. Plant Physiol 135, 212-220.

Hibara, K., Takada, S., and Tasaka, M. (2003). CUC1 gene activates the expression of SAM-related genes to induce adventitious shoot formation. Plant J 36, 687-696.

Hiratsu, K., Matsui, K., Koyama, T., and Ohme-Takagi, M. (2003). Dominant repression of target genes by chimeric repressors that include the EAR motif, a repression domain, in Arabidopsis. Plant J 34, 733-739.

Huntley, R., Healy, S., Freeman, D., Lavender, P., de Jager, S., Greenwood, J., Makker, J., Walker, E., Jackman, M., Xie, Q., Bannister, A.J., Kouzarides, T., Gutierrez, C., Doonan, J.H., and Murray, J.A. (1998). The maize retinoblastoma protein homologue ZmRb-1 is regulated during leaf development and displays conserved interactions with G1/S regulators and plant cyclin D (CycD) proteins. Plant Mol Biol 37, 155-169.

Kikuchi, K., Ueguchi-Tanaka, M., Yoshida, K.T., Nagato, Y., Matsusoka, M., and Hirano, H.Y. (2000). Molecular analysis of the NAC gene family in rice. Mol Gen Genet 262, 1047-1051.

Kubo, M., Udagawa, M., Nishikubo, N., Horiguchi, G., Yamaguchi, M., Ito, J., Mimura, T., Fukuda, H., and Demura, T. (2005). Transcription switches for protoxylem and metaxylem vessel formation. Genes Dev 19, 1855-1860.

Larson, P.R., and Isebrands, J.G. (1971). The plastochron index as applied to developmental studies in cottonwood. Can. J. For. Res. 1, 1-11.

Livak, K.J., and Schmittgen, T.D. (2001). Analysis of relative gene expression data using real-time quantitative PCR and the 2(-Delta Delta C(T)) Method. Methods 25, 402-408.

Maere, S., De Bodt, S., Raes, J., Casneuf, T., Van Montagu, M., Kuiper, M., and Van de Peer, Y. (2005). Modeling gene and genome duplications in eukaryotes. Proc Natl Acad Sci U S A 102, 5454-5459.

Meilan, R., and Ma, C. (2006). Poplar (Populus spp.). Methods Mol Biol 344, 143-151.

Menges, M., Samland, A.K., Planchais, S., and Murray, J.A. (2006). The D-type cyclin CYCD3;1 is limiting for the G1-to-S-phase transition in Arabidopsis. Plant Cell 18, 893-906.

Mitsuda, N., Seki, M., Shinozaki, K., and Ohme-Takagi, M. (2005). The NAC transcription factors NST1 and NST2 of Arabidopsis regulate secondary wall thickenings and are required for anther dehiscence. Plant Cell 17, 2993-3006.

Mitsuda, N., Iwase, A., Yamamoto, H., Yoshida, M., Seki, M., Shinozaki, K., and Ohme-Takagi, M. (2007). NAC transcription factors, NST1 and NST3, are key regulators of the formation of secondary walls in woody tissues of Arabidopsis. Plant Cell 19, 270-280.

Ohta, M., Matsui, K., Hiratsu, K., Shinshi, H., and Ohme-Takagi, M. (2001). Repression domains of class II ERF transcriptional repressors share an essential motif for active repression. Plant Cell 13, 1959-1968.

Olsen, A.N., Ernst, H.A., Leggio, L.L., and Skriver, K. (2005). NAC transcription factors: structurally distinct, functionally diverse. Trends Plant Sci 10, 79-87.

Ooka, H., Satoh, K., Doi, K., Nagata, T., Otomo, Y., Murakami, K., Matsubara, K., Osato, N., Kawai, J., Carninci, P., Hayashizaki, Y., Suzuki, K., Kojima, K., Takahara, Y., Yamamoto, K., and Kikuchi, S. (2003). Comprehensive

analysis of NAC family genes in Oryza sativa and Arabidopsis thaliana. DNA Res 10, 239-247.

Riechmann, J.L., Heard, J., Martin, G., Reuber, L., Jiang, C., Keddie, J., Adam, L., Pineda, O., Ratcliffe, O.J., Samaha, R.R., Creelman, R., Pilgrim, M., Broun, P., Zhang, J.Z., Ghandehari, D., Sherman, B.K., and Yu, G. (2000). Arabidopsis transcription factors: genome-wide comparative analysis among eukaryotes. Science 290, 2105-2110.

Sainz, M.B., Goff, S.A., and Chandler, V.L. (1997). Extensive mutagenesis of a transcriptional activation domain identifies single hydrophobic and acidic amino acids important for activation in vivo. Mol Cell Biol 17, 115-122.

Souer, E., van Houwelingen, A., Kloos, D., Mol, J., and Koes, R. (1996). The no apical meristem gene of Petunia is required for pattern formation in embryos and flowers and is expressed at meristem and primordia boundaries. Cell 85, 159-170.

Takada, S., Hibara, K., Ishida, T., and Tasaka, M. (2001). The CUP-SHAPED COTYLEDON1 gene of Arabidopsis regulates shoot apical meristem formation. Development 128, 1127-1135.

Thornton, C.R., and Talbot, N.J. (2006). Immunofluorescence microscopy and immunogold EM for investigating fungal infection of plants. Nat Protoc 1, 2506-2511.

Tuskan, G.A., Difazio, S., Jansson, S., Bohlmann, J., Grigoriev, I., Hellsten, U., Putnam, N., Ralph, S., Rombauts, S., Salamov, A., Schein, J., Sterck, L., Aerts, A., Bhalerao, R.R., Bhalerao, R.P., Blaudez, D., Boerjan, W., Brun, A., Brunner, A., Busov, V., Campbell, M., Carlson, J., Chalot, M., Chapman, J., Chen, G.L., Cooper, D., Coutinho, P.M., Couturier, J., Covert, S., Cronk, Q., Cunningham, R., Davis, J., Degroeve, S., Dejardin, A., Depamphilis, C., Detter, J., Dirks, B., Dubchak, I., Duplessis, S., Ehlting, J., Ellis, B., Gendler, K., Goodstein, D., Gribskov, M., Grimwood, J., Groover, A., Gunter, L., Hamberger, B., Heinze, B., Helariutta, Y., Henrissat, B., Holligan, D., Holt, R., Huang, W., Islam-Faridi, N., Jones, S., Jones-Rhoades, M., Jorgensen, R., Joshi, C., Kangasjarvi, J., Karlsson, J., Kelleher, C., Kirkpatrick, R., Kirst, M., Kohler, A., Kalluri, U., Larimer, F., Leebens-Mack, J., Leple, J.C., Locascio, P., Lou, Y., Lucas, S., Martin, F., Montanini, B., Napoli, C., Nelson, D.R., Nelson, C., Nieminen, K., Nilsson, O., Pereda, V., Peter, G., Philippe, R., Pilate, G., Poliakov, A., Razumovskaya, J., Richardson, P., Rinaldi, C., Ritland, K., Rouze, P., Ryaboy, D., Schmutz, J., Schrader, J., Segerman, B., Shin, H., Siddiqui, A., Sterky, F., Terry, A., Tsai, C.J., Uberbacher, E., Unneberg, P., Vahala, J., Wall, K., Wessler, S., Yang, G., Yin, T., Douglas, C., Marra, M., Sandberg, G., Van de Peer, Y., and Rokhsar, D. (2006). The genome of black cottonwood, Populus trichocarpa (Torr. & Gray). Science 313, 1596-1604.

van Engelen, F.A., Molthoff, J.W., Conner, A.J., Nap, J.P., Pereira, A., and Stiekema, W.J. (1995). pBINPLUS: an improved plant transformation vector based on pBIN19. Transgenic Res 4, 288-290.

Vroemen, C.W., Mordhorst, A.P., Albrecht, C., Kwaaitaal, M.A., and de Vries, S.C. (2003). The CUP-SHAPED COTYLEDON3 gene is required for boundary and shoot meristem formation in Arabidopsis. Plant Cell 15, 1563-1577.

Wan, X., Landhausser, S.M., Lieffers, V.J., and Zwiazek, J.J. (2006). Signals controlling root suckering and adventitious shoot formation in aspen (Populus tremuloides). Tree Physiol 26, 681-687.

Wu, L., Joshi, C.P., and Chiang, V.L. (2000). A xylem-specific cellulose synthase gene from aspen (Populus tremuloides) is responsive to mechanical stress. Plant J 22, 495-502.

Xie, Q., Frugis, G., Colgan, D., and Chua, N.H. (2000). Arabidopsis NAC1 transduces auxin signal downstream of TIR1 to promote lateral root development. Genes Dev 14, 3024-3036.

Yamaguchi, M., Kubo, M., Fukuda, H., and Demura, T. (2008). Vascular-related NAC-DOMAIN7 is involved in the differentiation of all types of xylem vessels in Arabidopsis roots and shoots. Plant J 55, 652-664.

Zhao, C., Johnson, B.J., Kositsup, B., and Beers, E.P. (2000). Exploiting secondary growth in Arabidopsis. Construction of xylem and bark cDNA libraries and cloning of three xylem endopeptidases. Plant Physiol 123, 1185-1196.

Zhao, C., Craig, J.C., Petzold, H.E., Dickerman, A.W., and Beers, E.P. (2005). The xylem and phloem transcriptomes from secondary tissues of the Arabidopsis root-hypocotyl. Plant Physiol 138, 803-818.

Zhao, C., Avci, U., Grant, E.H., Haigler, C.H., and Beers, E.P. (2008). XND1, a member of the NAC domain family in Arabidopsis thaliana, negatively regulates lignocellulose synthesis and programmed cell death in xylem. Plant J 53, 425-436.

Zimmermann, P., Hennig, L., and Gruissem, W. (2005). Gene-expression analysis and network discovery using Genevestigator. Trends Plant Sci 10, 407-409.

Appendix

Appendix Table I. **Linker primers used for amplification of selected *NAC* genes**

Primer	Sequence (5'-3')	Orientation	5' Site	Purpose
SRDX-S	*GGATCC*CCCGGGCTAGATCTGGATCTAGAACTC	Sense	*Sma* I	EAR Repressor Domain
SRDX-AS	ATTTAAATTTAAGCGAAACCCAAACGGAG	Antisense	*Swa* I	
ANAC073-S	CTCGAGATGACTTGGTGCAATGACCGT	Sense	*Xho* I	At4g28500
ANAC073-AS	ATTTAAATAAAGGGATAAAAGGTTGAGAGT	Antisense	*Swa* I	At4g28500 – antisense without stop codon
ANAC073-3	GATATCTTAAGGGATAAAAGGTTGAGAGT	Antisense	*Eco*R V	At4g28500 – antisense with stop codon
ANAC096-S	GTCGACATGGGAAGTTCATGTTTACCTC	Sense	*Sal* I	At5g46590
ANAC096-AS	ATTTAAATGAGGAGAAATCTGAGTAACCG	Antisense	*Swa* I	At5g46590 – antisense without stop codon
ANAC096-3	GATATCCTAGGAGAAATCTGAGTAACC	Antisense	*Eco*R V	At5g46590 – with stop Codon
PopNAC154-S	CTCGAGATGACTTGGTGCAATGACTGC	Sense	*Xho* I	*PopNAC154*; 3' RACE for *PopNAC156*
PopNAC154-AS	ATTTAAATGAGGGGATAAAAGAAGATCCA	Antisense	*Swa* I	*PopNAC154* – without stop Codon
PopNAC154-3	GATATCTCAGGGGATAAAAGAAGATCCA	Antisense	*Eco*R V	*PopNAC154* – with stop Codon
*NAC129*P1	CTCGAGATGGGAGATCATGGCTGCAG	Sense	*Xho* I	*PopNAC129* – sense
*NAC129*P4	GATATCACGAACCGAAGCACTCCAC	Antisense	*Eco*R V	*PopNAC129* – with stop Codon
*NAC129*P3	GATATCATTTGGAAAACTTATATCATCAAGAT	Antisense	*Eco*R V	*PopNAC129* and *122* – without stop codon
*Pa122*S	CTCGAGGGCTTCTGTTGATTAGACATG	Sense	*Xho* I	*PopNAC122*
*Pa122*AS	GATATCAGCCGAAACAATACTCAGAAAC	Antisense	*Eco*R V	*PopNAC122* – with stop Codon

VND7-S	CTCGAGATGGATAATATAATGCAATCGTC	Sense	*Xho* I	*AtVND7*
VND7-3	GATATCCGAGTCAGGGAAGCATCCA	Antisense	*Eco*R V	*AtVND7* – without stop codon
XND1N5-S	CTCGAGATGAATCTACCACCGGGATTT	Sense	*Xho* I	*AtXND1* – NAC Domain
XND1N5-AS	CAGCTGCTCATACACTCTGCATATCAC	Antisense	*Pvu* II	*AtXND1* - NAC Domain
XND1C-S	GTTAACTGCAGTGAGGAGGAAGACGA	Sense	*Hpa* I	*AtXND1* - C-terminus
XND1-02	GATATCTTACGGTAAGCTTACTTCGTC	Antisense	*Eco*R V	*AtXND1* – C-terminus
VND7AD-S	GTTAACACATCCTCATCGATGCATCAAT	Sense	*Hpa* I	*AtVND7* – activation domain
VND7AD-AS	GATATCTTACGAGTCAGGGAAGCATC	Antisense	*Eco*R V	*AtVND7* – activation domain
VP16-S	CTACTGATTTTTCCTAGGTCGGGC	Sense	*Sfo* I (partial site)	HSV - VP16 activation domain
VP16-AS	GATATCCTACCCACCGTACTCGTCA	Antisense	*Eco*R V	HSV – VP16 activation domain
3'RACE adapter	GAGACTCGAGTCGACATCG	Antisense	n/a	3' RACE
Pt118-Fwd1	CAATGGTTGGCCACGTTG	Sense	n/a	3' RACE for *PopNAC118*
Pt118-Fwd2	CCTTCTCTCGGAACATCGCACC	Sense	n/a	3' RACE nested primer for *PopNAC118*
Pt122-Fwd1	GATGGAGAACCAAGCAACAGG	Sense	n/a	3' RACE for *PopNAC122*
Pt122-Fwd2	GTACTGCATTGGTCCCGAAG	Sense	n/a	3' RACE nested primer for *PopNAC122*
Pt128-Fwd1	CGTGGCGAAGAGCTTGTG	Sense	n/a	3' RACE for *PopNAC128*
Pt128-Fwd2	GGAAGAGTACAGACTATCAGG	Sense	n/a	3' RACE nested primer for *PopNAC128*
Pt129-Fwd3	CTCTTACCTTGCAACCCTGAC	Sense	n/a	3' RACE for *PopNAC129*

Pt105-Fwd3	CTTTGCTTGTCTCCGCAGCTAATCT	Antisense	n/a	3' RACE for *PopNAC105*
Pt105-Fwd5	CAAGTGAGAGAACAATGGAGGTG	Sense	n/a	3' RACE for *PopNAC105*
Pt154-Fwd1	CTATGGGAAGCAAAGGAAGCCAGAG	Sense	n/a	3' RACE for *PopNAC154*
Pt154NFwd2	GTAGTGGGCATGAGGGCTCTAAC	Sense	n/a	3' RACE for *PopNAC154*
Pt154Rev2	TGCTACATGAGCCACCATATCATGCA	Antisense	n/a	3' RACE for *PopNAC154*
Pt156Rev1	TCAATGATTGCAGCCTTACTTTCCCA	Antisense	n/a	3' RACE for *PopNAC156*
Pt157-Fwd3	AGTACAGGCCTCCTTGAGTTCT	Antisense	n/a	3' RACE for *PopNAC157*
aUBQ2-F03	TGTACTCTTTTGAAGTTGGTGT	Sense	n/a	Real-Time PCR control
aUBQ2-R03	TCCAATGGAACGGCCATTAA	Antisense	n/a	Real-Time PCR control
Pt154q-Fwd	TCTTGCTGAGTACTATCACCCTTCTTC	Sense	n/a	Real-Time PCR
Pt154q-Rev	GCTACATGAGCCACCATATCATG	Antisense	n/a	Real-Time PCR
Pt156q-Fwd	GTACCACTCCTGTCGACTACTATAATCC	Sense	n/a	Real-Time PCR
Pt156q-Rev	TCACCAAGGCTCAATGATTGC	Antisense	n/a	Real-Time PCR
Pt118q-Fwd	GGGTCTATGAGCGGAGTTGTGAG	Sense	n/a	Real-Time PCR
Pt118q-Rev	CTAGCCTCCACAAATAAGTTGAGGAC	Antisense	n/a	Real-Time PCR
Pt122q-Fwd	CTGTTCCAGGAGTTTAAACCACAGTAG	Sense	n/a	Real-Time PCR
Pt122q-Rev	CACATGATTCATTAACATATAAGCCGAAAC	Antisense	n/a	Real-Time PCR
Pt128q-Fwd	CGAGTCTACGAGCGAGATCTTGAC	Sense	n/a	Real-Time PCR
Pt128q-Rev	CAAAGCCACAAAGGCGACAAC	Antisense	n/a	Real-Time PCR
Pt129q-Fwd	GCAGGAATATCATCTTTGCAACAG	Sense	n/a	Real-Time PCR
Pt129q-Rev	CGTCATCATCATCAGAGGTATTGC	Antisense	n/a	Real-Time PCR
Pt105q-Fwd	TGCATGGTTGTTGCTGTTGG	Sense	n/a	Real-Time PCR
Pt105q-Rev	CAAAGGCTTCCTTCCTACGATC	Antisense	n/a	Real-Time PCR

Pt157q-Fwd2	CGAGTGCATGGTTGTTGCTTC	Sense	n/a	Real-Time PCR
Pt157q-Rev2	ACGGCAAAGCTTCCAAAGAAC	Antisense	n/a	Real-Time PCR
XND1q-Fwd	CAAGTGGGTGATATGCAGAGTGTATG	Sense	n/a	Real-Time PCR
OCSTermq-Rev	GCGTCTCGCATATCTCATTAAAGC	Antisense	n/a	Real-Time PCR
OCSF	TATGCGAGACGCCTATGATCGCAT	Sense	n/a	Real-Time PCR
OCS102R	AGAATGAACCGAAACCGGCGGTAA	Antisense	n/a	Real-Time PCR

Table II. Ct values for *XND1 PopNAC* group tissue survey

Gene	Tissue	AVE Ct	STDEV	UBQ AVE Ct	UBQ STDEV	RQ	STD DEV
PopNAC122	Nodes 2-6	27.0290	0.0506	18.6154	0.1107	5.8853	0.2079
	Nodes 7-12	23.2610	0.0270	18.1556	0.0407	58.2972	1.0840
	LPI 1 Leaf	25.8370	0.0477	18.2169	0.0506	10.2001	0.3384
	LPI 3 Leaf	27.2389	0.0924	18.3434	0.0859	4.2140	0.2745
	LPI 6 Leaf	27.1506	0.0457	18.9708	0.0395	6.9205	0.2205
	Shoot Tip	26.4306	0.0938	18.6596	0.0719	9.1878	0.5977
	Internodes 2-3	29.0261	0.1487	18.0555	0.0429	1.0000	0.1022
	Internodes 5-6	24.1914	0.0821	17.9351	0.0696	26.2537	1.5040
	Xylem	22.7852	0.0893	18.2978	0.0624	89.4644	5.4231
	Bark	22.9182	0.0376	18.6932	0.1554	107.3082	2.7989
	Phloem-Cambium	22.9347	0.0793	19.9700	0.0498	257.0557	14.4291
	Root	22.9910	0.0492	18.1646	0.0630	70.7285	2.4441
	Floral Bud	25.7971	0.1268	17.5926	0.0676	6.8030	0.6219
PopNAC129	Nodes 2-6	25.6585	0.3176	18.6154	0.1107	5.0874	1.0763
	Nodes 7-12	23.8612	0.8851	18.1556	0.0407	12.8566	8.2222
	LPI 1 Leaf	17.7681	0.8511	18.2169	0.0506	915.7125	563.7390
	LPI 3 Leaf	27.7334	2.4657	18.3434	0.0859	1.0000	2.4038
	LPI 6 Leaf	27.2014	1.9008	18.9708	0.0395	2.2335	3.6088
	Shoot Tip	19.7259	0.9821	18.6596	0.0719	320.4002	230.8265
	Internodes 2-3	24.0221	1.1667	18.0555	0.0429	10.7280	14.2550
	Internodes 5-6	23.5854	0.7355	17.9351	0.0696	13.3591	7.0413
	Xylem	26.7833	1.7135	18.2978	0.0624	1.8719	2.6377
	Bark	24.2345	0.2163	18.6932	0.1554	14.4064	2.1283
	Phloem-Cambium	22.5896	1.1023	19.9700	0.0498	109.1661	89.6627
	Root	22.4533	1.1327	18.1646	0.0630	34.3269	29.0852
	Floral Bud	20.8126	1.0253	17.5926	0.0676	71.9977	54.1254
PopNAC118	Nodes 2-6	23.1116	0.0734	18.8384	0.1131	20.1963	1.0483
	Nodes 7-12	22.4146	0.0507	18.4564	0.2406	25.1231	0.8927
	LPI 1 Leaf	24.5444	0.1072	18.2197	0.1991	4.8718	0.3602
	LPI 3 Leaf	25.5935	0.1293	18.5927	0.1003	3.0491	0.2726

	LPI 6 Leaf	27.6836	0.1195	19.0744	0.0895	1.0000	0.0840
	Shoot Tip	23.9693	0.0533	18.9207	0.1254	11.7991	0.4382
	Internodes 2-3	24.8258	0.2149	18.1609	0.0315	3.8484	0.5631
	Internodes 5-6	26.8079	0.1259	18.3840	0.5089	1.1370	0.0985
	Xylem	26.1486	0.0441	18.5500	0.0905	2.0147	0.0608
	Bark	24.8042	0.1271	18.8623	0.1466	6.3525	0.5564
	Phloem-Cambium	28.0490	0.2281	20.0124	0.2255	1.4872	0.2363
	Root	23.6819	0.0620	18.3477	0.0841	9.6798	0.4198
	Floral Bud	22.6814	0.0853	17.8489	0.1001	13.7055	0.7994
PopNAC128	Nodes 2-6	24.9565	0.1072	18.8384	0.1131	92.5082	6.8525
	Nodes 7-12	25.3839	0.0629	18.4564	0.2406	52.7859	2.2888
	LPI 1 Leaf	22.7614	0.1906	18.2197	0.1991	275.8791	34.7846
	LPI 3 Leaf	22.3508	0.0939	18.5927	0.1003	474.9000	30.2648
	LPI 6 Leaf	23.5853	0.1213	19.0744	0.0895	281.8350	23.0108
	Shoot Tip	23.4857	0.0447	18.9207	0.1254	271.4732	8.3747
	Internodes 2-3	24.2396	0.0662	18.1609	0.0315	95.0709	4.4183
	Internodes 5-6	26.6129	0.0904	18.3840	0.5089	21.4164	1.3782
	Xylem	25.5870	0.1062	18.5500	0.0905	48.9290	3.6025
	Bark	31.5120	0.2973	18.8623	0.1466	1.0000	0.2109
	Phloem-Cambium	29.7994	0.3164	20.0124	0.2255	7.2733	1.6185
	Root	25.8933	0.1436	18.3477	0.0841	34.3926	3.4274
	Floral Bud	22.9194	0.0988	17.8489	0.1001	191.2194	13.4821

Table III. Ct values for *ANAC073 PopNAC* group tissue survey

Gene	Tissue	AVE Ct	STDEV	UBQ AVE Ct	UBQ STDEV	RQ	STD DEV
PopNAC156	Nodes 2-6	22.4510	0.0430	17.5586	0.0775	3.4625	0.1023
	Nodes 7-12	19.8128	0.0219	17.3749	0.0880	18.9493	0.2888
	LPI 1 Leaf	21.9009	0.0662	17.6690	0.2939	5.4641	0.2506
	LPI 3 Leaf	21.3281	0.0571	17.4968	0.0464	7.2131	0.2852
	LPI 6 Leaf	22.6826	0.1011	18.1057	0.0690	4.3022	0.3014
	Shoot Tip	22.2731	0.0527	18.0127	0.0737	5.3572	0.1942
	Internodes 2-3	21.5879	0.0908	17.2698	0.0080	5.1472	0.3178
	Internodes 5-6	18.7301	0.1182	17.2060	0.0247	35.6977	3.0127
	Xylem	17.5611	0.1451	17.4501	0.0570	95.0721	9.5721
	Bark	22.5171	0.0514	17.7442	0.0614	3.7557	0.1321
	Phloem-Cambium	24.3876	0.3125	26.7777	0.1878	2.8835	0.1927
	Root	29.4148	0.0967	19.2335	0.0534	16.5051	3.7882
	Floral Bud	23.8075	0.1624	17.1256	0.0313	1.0000	0.1117
PopNAC154	Nodes 2-6	23.2123	0.2250	17.5586	0.0775	3.1989	0.5260
	Nodes 7-12	19.9894	0.2140	17.3749	0.0880	26.4236	3.9287
	LPI 1 Leaf	22.6191	0.1818	17.6690	0.2939	5.2346	0.6327
	LPI 3 Leaf	22.0453	0.3294	17.4968	0.0464	6.9155	1.5750
	LPI 6 Leaf	23.2593	0.2613	18.1057	0.0690	4.5461	0.8404
	Shoot Tip	23.1074	0.2169	18.0127	0.0737	4.7355	0.7220
	Internodes 2-3	22.2431	0.2422	17.2698	0.0080	5.1514	0.8778

	Internodes 5-6	18.9526	0.2984	17.2060	0.0247	48.2231	10.0039
	Xylem	17.1737	0.2137	17.4501	0.0570	195.9910	29.4055
	Bark	21.9564	0.2411	17.7442	0.0614	8.7303	1.4822
	Phloem-Cambium	23.7796	0.6354	19.2335	0.1878	6.9266	1.0492
	Root	29.6526	0.2104	26.7777	0.0534	22.0597	10.2125
	Floral Bud	24.4638	0.4096	17.1256	0.0313	1.0000	0.2777
PopNAC157	Nodes 2-6	23.8683	0.0910	18.5227	0.0964	1.0435	0.0670
	Nodes 7-12	22.1678	0.0817	18.0723	0.0726	2.4821	0.1420
	LPI 1 Leaf	23.4770	0.0710	18.2763	0.0541	1.1538	0.0571
	LPI 3 Leaf	22.8885	0.1126	18.3394	0.0305	1.8126	0.1404
	LPI 6 Leaf	22.7778	0.0827	18.8173	0.1063	2.7256	0.1599
	Shoot Tip	24.0497	0.1754	18.6426	0.1006	1.0000	0.1210
	Internodes 2-3	23.0958	0.0289	17.8330	0.0750	1.1010	0.0220
	Internodes 5-6	21.6727	0.1188	17.9665	0.0728	3.2511	0.2634
	Xylem	20.5887	0.0625	18.2173	0.0724	8.2004	0.3549
	Bark	22.8720	0.0974	18.5980	0.0625	2.1932	0.1467
	Phloem-Cambium	23.7541	0.1942	19.9812	0.0847	3.1040	0.4131
	Root	22.3279	0.1533	18.2140	0.1111	2.4506	0.2544
	Floral Bud	22.5957	0.1156	17.5955	0.0156	1.3258	0.1032
PopNAC105	Nodes 2-6	24.4594	0.0789	18.5227	0.0964	4.8529	0.2666
	Nodes 7-12	22.3465	0.0515	18.0723	0.0726	15.3624	0.5406
	LPI 1 Leaf	25.6588	0.1490	18.2763	0.0541	1.7815	0.1775
	LPI 3 Leaf	24.4587	0.1630	18.3394	0.0305	4.2762	0.4620
	LPI 6 Leaf	24.5680	0.0953	18.8173	0.1063	5.5209	0.3647
	Shoot Tip	26.8582	0.2520	18.6426	0.1006	1.0000	0.1913
	Internodes 2-3	22.9115	0.0702	17.8330	0.0750	8.7973	0.4355
	Internodes 5-6	22.0625	0.0543	17.9665	0.0728	17.3835	0.6649
	Xylem	20.9403	0.0989	18.2173	0.0724	45.0248	3.1452
	Bark	22.8829	0.0639	18.5980	0.0625	15.2492	0.6731
	Phloem-Cambium	23.0634	0.0402	18.2140	0.0847	35.0997	0.9749
	Root	23.2832	0.0446	19.9812	0.1111	8.8539	0.2743
	Floral Bud	23.8436	0.1924	17.5955	0.0156	3.9109	0.5257

Table IV. Ct values for *XND1 PopNAC* group for developmental gradient

Gene	Tissue	AVE Ct	STDEV	UBQ AVE Ct	UBQ STDEV	RQ	STD DEV
PopNAC122	2,3 Internode	26.1767	0.0615	17.7309	0.1169	1.7714	0.0764
	4,5 Internode	26.1160	0.0788	17.5836	0.0995	1.6681	0.0935
	6,7 Internode	24.1558	0.0345	17.5774	0.0528	6.4635	0.1555
	8-10 Internode	23.8166	0.0400	17.8914	0.1044	10.1645	0.2804
	Xylem	24.9088	0.0320	18.5225	0.1514	7.3837	0.1643
	Bark	24.1343	0.0733	17.7770	0.0759	7.5337	0.3828
	Phloem-Cambium	23.7310	0.0322	18.1157	0.0907	12.6003	0.2782
	LPI 1	27.6316	0.0628	18.3609	0.1137	1.0000	0.0444
	LPI 3	27.2030	0.0726	19.3554	0.0489	2.6815	0.1372

	LPI 6	27.6042	0.1516	19.8004	0.0736	2.7643	0.2992
PopNAC129	2,3 Internode	22.9960	0.1079	17.8259	0.1506	136.1615	9.9565
	4,5 Internode	22.2978	0.1096	17.7069	0.1004	203.4295	14.9651
	6,7 Internode	23.5552	0.1053	17.6429	0.1092	81.3989	5.8416
	8-10 Internode	24.1925	0.0477	17.9209	0.1578	63.4542	2.1009
	Xylem	28.9217	0.1562	18.5447	0.0803	3.6867	0.3953
	Bark	23.4445	0.0646	17.8112	0.1212	98.7645	4.4211
	Phloem-Cambium	23.8120	0.0971	18.1160	0.1164	94.5714	6.3760
	LPI 1	30.6829	0.1401	18.4236	0.0881	1.0000	0.0964
	LPI 3	29.3523	0.2299	19.3792	0.0734	4.8777	0.7846
	LPI 6	29.3763	0.2198	19.8639	0.0925	6.7125	0.9521
PopNAC118	2,3 Internode	23.5931	0.1302	17.7309	0.1169	3.7170	0.3488
	4,5 Internode	24.3690	0.1825	17.5836	0.0995	1.9600	0.2349
	6,7 Internode	25.3337	0.0406	17.5774	0.0528	1.0000	0.0280
	8-10 Internode	25.5128	0.0464	17.8914	0.1044	1.0980	0.0351
	Xylem	24.8284	0.0305	18.5225	0.1514	2.7328	0.0579
	Bark	24.8598	0.0851	17.7770	0.0759	1.5949	0.0963
	Phloem-Cambium	24.5358	0.1238	18.1157	0.0907	2.5247	0.2243
	LPI 1	23.8787	0.0858	18.3609	0.1137	4.7191	0.2866
	LPI 3	23.9424	0.1114	19.3554	0.0489	8.9958	0.6811
	LPI 6	24.9801	0.1248	19.8004	0.0736	5.9653	0.5025
PopNAC128	2,3 Internode	23.6013	0.0584	17.7309	0.1169	77.4200	3.1569
	4,5 Internode	25.0233	0.0863	17.5836	0.0995	26.0866	1.5366
	6,7 Internode	25.4057	0.0807	17.5774	0.0528	19.9276	1.1165
	8-10 Internode	24.9712	0.0564	17.8914	0.1044	33.4786	1.2995
	Xylem	25.6819	0.1217	18.5225	0.1514	31.6805	2.7361
	Bark	29.9220	0.3027	17.7770	0.0759	1.0000	0.2026
	Phloem-Cambium	29.0582	0.0740	18.1157	0.0907	2.3013	0.1161
	LPI 1	21.7272	0.0696	18.3609	0.1137	439.2042	21.2216
	LPI 3	20.7451	0.1176	19.3554	0.0489	1728.4358	139.5851
	LPI 6	23.2746	0.0609	19.8004	0.0736	407.5215	17.3765

Table V. Ct values for *ANAC073 PopNAC* group for developmental gradient

Gene	Tissue	AVE Ct	STDEV	UBQ AVE Ct	UBQ STDEV	RQ	STD DEV
PopNAC156	2,3 Internode	21.0391	0.0538	17.8259	0.1506	6.2256	0.2299
	4,5 Internode	18.8838	0.0843	17.7069	0.1004	25.5373	1.4686
	6,7 Internode	18.5893	0.0388	17.6429	0.1092	29.9616	0.8042
	8-10 Internode	18.6267	0.0517	17.9209	0.1578	35.3978	1.2702
	Xylem	17.1767	0.0392	18.5447	0.0803	149.0301	4.0362
	Bark	22.3481	0.0665	17.8112	0.1212	2.4871	0.1157
	Phloem-Cambium	23.9675	0.0456	18.1160	0.1164	1.0000	0.0317
	LPI 1	22.1236	0.0452	18.4236	0.0881	4.4429	0.1393
	LPI 3	22.1037	0.0409	19.3792	0.0734	8.7356	0.2474
	LPI 6	22.1535	0.0724	19.8639	0.0925	11.8093	0.5888

	2,3 Internode	21.7212	0.1889	17.8259	0.1506	2.1311	0.2638
	4,5 Internode	19.0915	0.1044	17.7069	0.1004	12.1447	0.8944
	6,7 Internode	18.6567	0.2771	17.6429	0.1092	15.7039	3.2729
	8-10 Internode	18.7811	0.1009	17.9209	0.1578	17.4687	1.2367
	Xylem	17.0716	0.0684	18.5447	0.0803	88.0374	4.0862
PopNAC154	Bark	21.1932	0.1475	17.8112	0.1212	3.0415	0.3112
	Phloem-Cambium	23.1029	0.0835	18.1160	0.1164	1.0000	0.0595
	LPI 1	22.9061	0.1078	18.4236	0.0881	1.4185	0.1075
	LPI 3	22.8919	0.0877	19.3792	0.0734	2.7782	0.1706
	LPI 6	23.0008	0.0976	19.8639	0.0925	3.6049	0.2508
	2,3 Internode	24.5419	0.1376	17.9402	0.1220	1.0000	0.0940
	4,5 Internode	22.9223	0.0639	17.6977	0.0917	2.5975	0.1148
	6,7 Internode	22.2226	0.0511	17.5976	0.0181	3.9359	0.1407
	8-10 Internode	22.0129	0.0851	17.9283	0.0251	5.7240	0.3386
	Xylem	20.6789	0.0510	18.3696	0.0729	19.5941	0.7000
PopNAC157	Bark	23.0442	0.0850	17.6990	0.0893	2.3890	0.1439
	Phloem-Cambium	23.6083	0.0713	17.9020	0.1245	1.8602	0.0917
	LPI 1	25.0574	0.1102	18.4851	0.0635	1.0206	0.0781
	LPI 3	24.7712	0.0852	19.3627	0.0751	2.2865	0.1367
	LPI 6	23.8836	0.1298	19.8278	0.0528	5.8395	0.5225
	2,3 Internode	24.0901	0.1530	17.9402	0.1220	3.2634	0.3487
	4,5 Internode	22.5567	0.1241	17.6977	0.0917	7.9854	0.6835
	6,7 Internode	22.3276	0.0284	17.5976	0.0181	8.7321	0.1734
	8-10 Internode	22.1499	0.0417	17.9283	0.0251	12.4210	0.3579
	Xylem	20.7176	0.1116	18.3696	0.0729	45.5180	3.5028
PopNAC105	Bark	22.9303	0.0512	17.6990	0.0893	6.1690	0.2173
	Phloem-Cambium	22.8416	0.0758	17.9020	0.1245	7.5513	0.3952
	LPI 1	26.3415	0.0973	18.4851	0.0635	1.0000	0.0665
	LPI 3	25.0513	0.0614	19.3627	0.0751	4.4929	0.1913
	LPI 6	24.7102	0.0833	19.8278	0.0528	7.8564	0.4602

Table VI. Ct values for *XND1 PopNAC* group in response to bending stress

Gene	Tissue	AVE Ct	STDEV	UBQ AVE Ct	UBQ STDEV	RQ	STD DEV
	Vertical Xylem	24.8527	0.0581	0.1145	19.2798	1.2706	0.0510
	Tension Xylem	24.1651	0.0740	0.1716	19.0231	1.7130	0.0864
	Opposite Xylem	23.4268	0.0727	0.1608	19.7024	4.5759	0.2274
PopNAC122	Vertical Phloem-Cambium	24.3745	0.1289	0.1507	20.0361	2.9897	0.2659
	Tension Phloem-Cambium	25.3500	0.0545	0.0254	19.5957	1.1205	0.0427
	Opposite Phloem-Cambium	25.9019	0.0734	0.0443	19.9834	1.0000	0.0505
PopNAC129	Vertical Xylem	30.0388	0.1845	19.2798	0.1145	1.0000	0.1307
	Tension Xylem	28.7453	0.0488	19.0231	0.1716	2.0517	0.0692
	Opposite Xylem	27.4200	0.0850	19.7024	0.1608	8.2330	0.4860
	Vertical Phloem-	24.1483	0.0221	20.0361	0.1507	100.2023	1.5227

	Cambium						
	Tension Phloem-Cambium	23.9971	0.0824	19.5957	0.0254	81.9999	4.6752
	Opposite Phloem-Cambium	24.3524	0.0550	19.9834	0.0443	83.8645	3.1853
PopNAC118	Vertical Xylem	25.4066	0.0747	19.2798	0.1145	2.0346	0.1055
	Tension Xylem	24.7410	0.0644	19.0231	0.1716	2.7013	0.1207
	Opposite Xylem	24.6792	0.1068	19.7024	0.1608	4.5152	0.3446
	Vertical Phloem-Cambium	27.0766	0.2795	20.0361	0.1507	1.0800	0.2152
	Tension Phloem-Cambium	26.5859	0.0777	19.5957	0.0254	1.1183	0.0611
	Opposite Phloem-Cambium	26.2438	0.1240	19.9834	0.0443	1.8548	0.1634
PopNAC128	Vertical Xylem	26.2204	0.0936	19.2798	0.1145	36.2860	2.3563
	Tension Xylem	28.3022	0.0649	19.0231	0.1716	7.1745	0.3168
	Opposite Xylem	26.7462	0.1879	19.7024	0.1608	33.7831	4.1775
	Vertical Phloem-Cambium	32.2109	0.5203	20.0361	0.1507	0.9640	0.3522
	Tension Phloem-Cambium	28.3341	0.1519	19.5957	0.0254	10.4365	1.1025
	Opposite Phloem-Cambium	27.2618	0.1184	19.9834	0.0443	28.7129	2.3233

Table VII. Ct values for *ANAC073 PopNAC* group in response to bending stress

Gene	Tissue	AVE Ct	STDEV	UBQ AVE Ct	UBQ STDEV	RQ	STD DEV
PopNAC156	Vertical Xylem	17.7756	0.1268	18.9384	0.1897	80.8934	7.0658
	Tension Xylem	18.7581	0.0312	18.8194	0.2443	37.6975	0.8139
	Opposite Xylem	19.0131	0.0519	19.3959	0.1301	47.1101	1.7041
	Vertical Phloem-Cambium	24.8994	0.0540	19.7238	0.1419	0.9997	0.0369
	Tension Phloem-Cambium	24.3663	0.0989	19.2646	0.0927	1.0523	0.0720
	Opposite Phloem-Cambium	24.4472	0.1277	19.5631	0.0908	1.2235	0.1093
PopNAC154	Vertical Xylem	17.5620	0.0830	18.9384	0.1897	49.7538	2.8259
	Tension Xylem	17.9281	0.0721	18.8194	0.2443	35.5485	1.7758
	Opposite Xylem	18.0309	0.1196	19.3959	0.1301	49.3647	4.1304
	Vertical Phloem-Cambium	23.9860	0.0128	19.7238	0.1419	0.9988	0.0089
	Tension Phloem-Cambium	23.4775	0.0538	19.2646	0.0927	1.0335	0.0390
	Opposite Phloem-Cambium	23.4452	0.0482	19.5631	0.0908	1.2998	0.0432
PopNAC157	Vertical Xylem	20.7840	0.1442	18.9384	0.1897	12.1218	1.1552
	Tension Xylem	21.2109	0.0421	18.8194	0.2443	8.3032	0.2451
	Opposite Xylem	21.1909	0.0475	19.3959	0.1301	12.5550	0.4066
	Vertical Phloem-Cambium	25.1724	0.0691	19.7238	0.1419	0.9977	0.0479
	Tension Phloem-	24.4048	0.0378	19.2646	0.0927	1.2355	0.0323

	Cambium						
	Opposite Phloem-Cambium	24.3351	0.0692	19.5631	0.0908	1.5946	0.0758
PopNAC105	Vertical Xylem	20.9637	0.1817	18.9384	0.1897	9.1378	1.1729
	Tension Xylem	21.0418	0.0643	18.8194	0.2443	7.9709	0.3541
	Opposite Xylem	21.8120	0.4672	19.3959	0.1301	6.9697	1.9669
	Vertical Phloem-Cambium	24.9185	0.0799	19.7238	0.1419	1.0157	0.0558
	Tension Phloem-Cambium	24.4399	0.1313	19.2646	0.0927	1.0295	0.0937
	Opposite Phloem-Cambium	24.5269	0.1104	19.5631	0.0908	1.1920	0.0914

Table VIII. Differences in overall size and cell size and number in *Pro$_{35S}$:XND1.14* versus WT

Plant	Overall Height	Diameter	Number of Internodes	Ave Internode Length	Ave Cells/File*	Ave Cell Size	Ave Vessel Frequency	Ray Frequency
Pro35S:XND1.14	10.2 cm	1.93 mm	17	0.6 cm	47.7	0.11 cm	1.68%	16%
Wild-Type	93.7 cm	7.14 mm	44	2.13 cm	62.5	0.22 cm	4.32%	26%

*p value<0.0001

Table IX. Ct values for *PopNAC154* in transgenic lines

Gene	Transgenic Event	AVE Ct	STDEV	UBQ AVE Ct	UBQ STDEV	RQ	STD DEV
PopNAC154	30D	18.7606	0.0571	20.6277	0.0988	40.3259	1.6097
	14C	19.1270	0.0303	20.8699	0.1539	37.0003	0.7807
	15D	18.7662	0.0818	20.4860	0.0898	36.4118	2.0935
	16C	21.1004	0.0435	20.9244	0.1739	9.7852	0.2967
	9C	20.2619	0.0685	19.9655	0.1372	9.0019	0.4229
	40A	36.5364	0.9811	36.1115	1.8037	8.2350	6.4049
	31A	21.2506	0.0498	20.6997	0.1748	7.5459	0.2621
	32C	21.2345	0.0741	20.1498	0.1646	5.2125	0.2700
	11G	22.1632	0.0873	19.5119	0.1382	1.7597	0.1056
	11C	23.8716	0.1203	20.4050	0.1158	1.0000	0.0827

Table X. Ct values for *Pro$_{35S}$:XND1* in *Populus* transgenic lines

Gene	Transgenic Event	AVE Ct	STDEV	UBQ AVE Ct	UBQ STDEV	RQ	STD DEV
XND1	1	15.8846	0.0711	19.6326	0.1959	1.2579	0.0612
	6	16.7830	0.0763	20.2176	0.1352	1.0123	0.0523
	7	15.8247	0.1553	19.5398	0.3143	1.2295	0.1322
	8	14.4636	0.1249	20.0601	0.1393	4.5302	0.3980
	11	15.3671	0.1676	20.4963	0.1351	3.2765	0.3780
	14	16.5979	0.1398	20.6254	0.1099	1.5268	0.1477